

Weierstraß-Institut
für Angewandte Analysis und Stochastik
Leibniz-Institut im Forschungsverbund Berlin e. V.

Preprint

ISSN 2198-5855

Coexistence of Hamiltonian-like and dissipative dynamics
in chains of coupled phase oscillators
with skew-symmetric coupling

Oleksandr Burylko¹, Alexander Mielke^{2,3}, Matthias Wolfrum², Serhiy Yanchuk⁴

submitted: November 8, 2017

¹ Institute of Mathematics
National Academy of Sciences of Ukraine
Tereshchenkivska Str. 3
01601 Kyiv
Ukraine
E-Mail: burylko@yahoo.co.uk

² Weierstrass Institute
Mohrenstr. 39
10117 Berlin
Germany
E-Mail: alexander.mielke@wias-berlin.de
matthias.wolfrum@wias-berlin.de

³ Institut für Mathematik
Humboldt-Universität zu Berlin
Rudower Chaussee 25
12489 Berlin
Germany

⁴ Technical University of Berlin
Institute of Mathematics
Straße des 17. Juni 136
10623 Berlin
Germany
E-Mail: yanchuk@math.tu-berlin.de

No. 2447

Berlin 2017



2010 *Mathematics Subject Classification.* 34C14, 34C15, 34C28, 34C30, 37C80, 37L60.

Key words and phrases. Phase oscillators, reversible systems, amplitude equations.

OB acknowledges financial support from Erasmus Mundus (Grant MID2012B895) for the work in Humboldt University. AM was partially supported by DFG within the Collaborative Research Center 910 through Project A5. MW and SY were partially supported by DFG within the Collaborative Research Center 910 through Project A3.

Edited by
Weierstraß-Institut für Angewandte Analysis und Stochastik (WIAS)
Leibniz-Institut im Forschungsverbund Berlin e. V.
Mohrenstraße 39
10117 Berlin
Germany

Fax: +49 30 20372-303
E-Mail: preprint@wias-berlin.de
World Wide Web: <http://www.wias-berlin.de/>

Coexistence of Hamiltonian-like and dissipative dynamics in chains of coupled phase oscillators with skew-symmetric coupling

Oleksandr Burylko, Alexander Mielke, Matthias Wolfrum, Serhiy Yanchuk

Abstract

We consider rings of coupled phase oscillators with anisotropic coupling. When the coupling is skew-symmetric, i.e. when the anisotropy is balanced in a specific way, the system shows robustly a coexistence of Hamiltonian-like and dissipative regions in the phase space. We relate this phenomenon to the time-reversibility property of the system. The geometry of low-dimensional systems up to five oscillators is described in detail. In particular, we show that the boundary between the dissipative and Hamiltonian-like regions consists of families of heteroclinic connections. For larger chains with skew-symmetric coupling, some sufficient conditions for the coexistence are provided, and in the limit of $N \rightarrow \infty$ oscillators, we formally derive an amplitude equation for solutions in the neighborhood of the synchronous solution. It has the form of a nonlinear Schrödinger equation and describes the Hamiltonian-like region existing around the synchronous state similarly to the case of finite rings.

1 Introduction

Many phenomena in nature can be studied using models of lattices of coupled oscillatory systems. Examples are interacting semiconductor lasers [56], neural networks [2, 47], mechanical systems [28], biological oscillators [58], and others. In the limit of weak coupling, the dynamics of each subsystem can be described by a scalar phase variable [26, 64], and the coupled system can be reduced to a lattice of phase oscillators. In this context, one dimensional arrays with periodic boundary conditions have been studied extensively [15, 51, 38, 58, 22, 17, 62, 69, 68, 42, 66, 30]. The rotation symmetry of such a system is a source of rich dynamical behavior including rotating waves [47, 70, 69, 8, 41, 45, 67, 68], heteroclinic cycles, symmetric chaos [16, 68, 42, 38, 70], chimera states [32, 1, 66], or compactons [43]. As an application in neuroscience, bifurcation mechanisms in rings of coupled Hodgkin-Huxley type neurons with inhibitory and excitatory synapses were studied in [7, 55, 27, 65], where a complex dynamical scenario and multistability are reported. A specific coupling structure on a ring is the case of undirected non-local coupling to several nearest neighbors, where self-organized patterns of coherence and incoherence, so called “chimera states”, have been discovered.

While for certain applications, such as molecular chains, the coupling of one element to its neighbors is symmetric with respect to reflection in space, for other systems the coupling is essentially directional. This happens for instance in laser systems with directional coupling through optical injection or in neuronal systems, where neurons are coupled in one direction via chemical synapses. As a result, there is a need for the theoretical understanding of the dynamical properties of rings with non-symmetric (anisotropic) couplings.

In this work we focus on a specific case of the anisotropy, when the coupling matrix is skew-symmetric. In such a case the system possesses a time-reversal symmetry, and the dynamics exhibits the coex-

istence of Hamiltonian-like and dissipative regions in the phase space for the same parameter values. Moreover, there can be more than one Hamiltonian-like "island", and the solutions in conservative region can be periodic, quasi-periodic, or chaotic. For some cases, the dynamics becomes conservative.

We remind that time-reversal symmetry \mathcal{R} of a system $\dot{x} = G(x)$ is the involution \mathcal{R} of the phase space satisfying

$$G(\mathcal{R}\Phi) = -\mathcal{R}(G(\Phi)) \quad (1.1)$$

and $\mathcal{R}^2 = id$, with id being the identical transformation. In particular, time-reversibility implies that $\mathcal{R}\Phi(-t)$ is a solution when $\Phi(t)$ is.

We note that there have been examples of reversible systems reported as well as the coexistence of Hamiltonian-like and dissipative dynamics in reversible systems. Politi et al. showed such dynamics in a 3-dimensional laser system [44]. Globally coupled superconducting Josephson junction arrays were studied by Tsang et al. [61] who showed the coexistence of Hamiltonian-like and dissipative dynamics, with the Hamiltonian-like dynamics being non-homotopic to zero. An infinite chain of locally coupled phase oscillators with reversible properties has been studied by Topaj and Pikovsky in [59], and an asymmetric ring by Pikovsky and Rosenau in [43]. The latter case corresponds to a particular case of our model (4.1), which will be introduced in Sec. 4. Golubitsky et al. proved the existence of families of periodic and quasi-periodic solutions in the Stokeslet model with time-reversal symmetry [23]. For general theoretical results on the dynamics of time-reversible systems, see [39, 18, 3, 52, 21, 33, 49, 20, 35, 6, 36, 71, 11, 9, 54], the review [34] by J. Lamb and references therein.

This paper is organized as follows. In Section 2 the model for the ring of coupled phase oscillators as well as the system for phase differences are introduced. In the following Sec. 3 we define synchronous solutions and rotating waves and provide conditions for their existence and asymptotic stability. In particular, we give explicit expressions for the eigenvalues of the characteristic equation for the rotating waves.

In Section 4 we consider a more specific example of a "forward-backward system", for which the coupling strengths to one or several next neighbors in one direction (forward) are all equal to the same value a , while in the other direction (backward) equally many next neighbors are coupled all with coupling strength b . In such a case, the anisotropy of the coupling can be measured by the difference $a - b$, and the skew-symmetric case corresponds to $a + b = 0$. We provide conditions for the bifurcations and, in particular, show that in the case where the coupling is skew-symmetric, i.e. $a + b = 0$, and includes only nearest-neighbors *all* eigenvalues of the rotating waves become purely imaginary.

In Section 5, global properties of low-dimensional (dimension $N = 3, 4$ and 5) forward-backward systems with a coupling function of Kuramoto-Sakaguchi type are studied in detail. It is shown that for $a + b = 0$ the phase space exhibits the coexistence of a Hamiltonian-like region and a dissipative region. For $N = 3$, the phase space for phase differences is two-dimensional, and the Hamiltonian-like region is foliated by a one-parameter family of periodic orbits bounded by a Z_3 -invariant heteroclinic cycle. For this case, a complete bifurcation diagram as well as a list of possible phase portraits are obtained. For the case $N = 4$ and $a + b = 0$, the Hamiltonian-like region in the neighborhood of the synchronous state is shown to be foliated by a 2-dimensional family of periodic orbits and bounded by a surface, which is composed of heteroclinic cycles. In these low-dimensional cases, the relation between the dimension of the subspace $\text{Fix } \mathcal{R}$ and the phase space dimension N is of importance. For $N = 4$, when the dimension of $\text{Fix } \mathcal{R}$ is 2, the complete global description of the phase space becomes complicated. Hence, the existence of an Hamiltonian-like region is shown only locally in the neighborhood of the synchronous state, while the existence of a dissipative region is shown in the neighborhood of asymptotically stable or unstable rotating waves. The sizes of the domains are

estimated numerically by calculating the Lyapunov exponents.

In Section 6 we consider a system with an arbitrary number N of coupled identical oscillators. This system is time-reversible for skew-symmetric coupling, and $\dim(\text{Fix } \mathcal{R}) = \lfloor N/2 \rfloor$ holds. We present conditions for the existence of a one-parameter family of periodic solutions when N is odd and conditions for the existence of a two-parameter family for N even, as well as conditions for the appearance of $\lfloor (N-1)/2 \rfloor$ -dimensional tori in the neighborhood of the synchronous solution. Hence, the main message is that the splitting of the phase space in a Hamiltonian-like region close to sync and a dissipative region still holds for the case of arbitrary N , though with less geometric insight compared to the cases of small N , studied before.

Section 7 considers specific cases when the reversible or conservative dynamics can occur in systems with non-identical coupled oscillators. We show that system with arbitrary frequency differences, skew-symmetric (resp. symmetric) coupling, and odd (resp. even) coupling function is divergence free, leading to the coexistence of periodic, quasiperiodic, and chaotic solutions. For some cases, the first integrals are computed. For a special constellation of natural frequencies (equally distributed) we show also the reversibility.

Finally, in Sec. 8 we consider the dynamics in a neighborhood of the synchronous solution in the case of an infinite chain of identical oscillators ($N \rightarrow \infty$) when each oscillator is coupled with a finite number $2l$ of its neighbors. In particular, we show that for the skew-symmetric coupling the resulting amplitude equation is the nonlinear Schrödinger equation. This fact agrees well with the observations for finite N , where, as we have shown, the neighborhood of the synchronous solution displays Hamiltonian-like dynamics. We conclude with a discussion in Sec. 9.

2 Oscillator model with circulant coupling

We consider the following translationally invariant chain of coupled phase oscillators with periodic boundary conditions

$$\dot{\theta}_i = \omega_i + \sum_{j=1}^N K_j g(\theta_i - \theta_{i+j}), \quad i = 1, \dots, N, \quad (2.1)$$

where $\theta_i \in [0, 2\pi)$ are phase variables, ω_i are natural frequencies, $g(x)$ is a smooth 2π -periodic coupling function, K_j , $j = 1, \dots, N$, are coupling strengths, and all subscripts are assumed modulo N . The coefficient $K_N \equiv K_0$ determines the self-coupling. System (2.1) can be rewritten in a way similar to the Kuramoto system [31] as follows

$$\dot{\theta}_i = \omega_i + \sum_{j=1}^N K_{j-i} g(\theta_i - \theta_j), \quad i = 1, \dots, N,$$

and it describes a network of oscillators with coupling strengths given by the *circulant* coupling matrix

$$K = \text{circ}(K_0, K_1, \dots, K_{N-1}) = \begin{pmatrix} K_0 & K_1 & \dots & K_{N-2} & K_{N-1} \\ K_{N-1} & K_0 & K_1 & \ddots & K_{N-2} \\ \vdots & K_{N-1} & K_0 & \ddots & \vdots \\ K_2 & \ddots & \ddots & \ddots & K_1 \\ K_1 & K_2 & \dots & K_{N-1} & K_0 \end{pmatrix}. \quad (2.2)$$

Figure 2.1 shows examples of networks with circulant connections for seven oscillators with coupling strengths K_0, \dots, K_6 . Note that system (2.1) reduces to the classical Kuramoto model of globally coupled oscillators when $K_i = K_0$ for all $i = 1, \dots, N - 1$ and $g(x) = \sin x$.

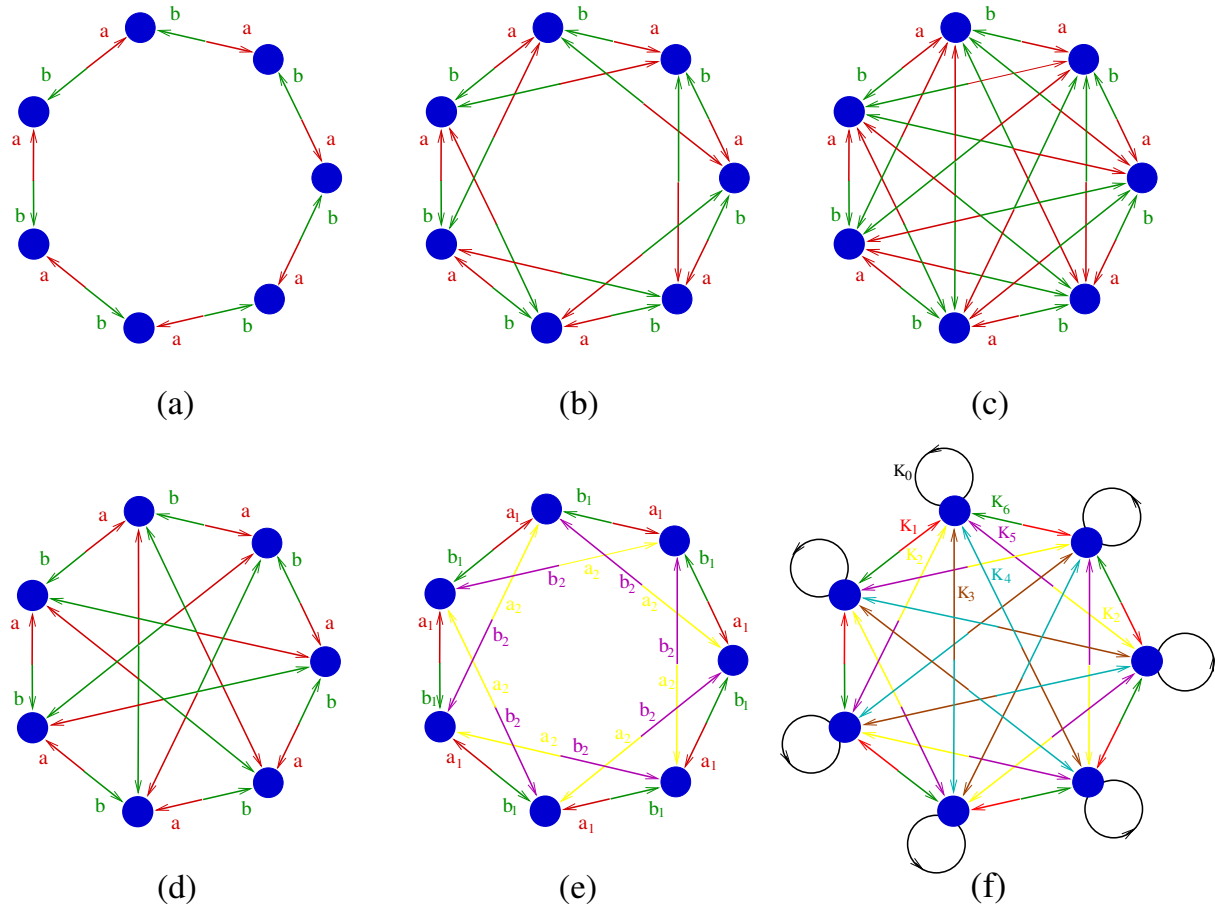


Figure 2.1: Networks of seven asymmetrically coupled oscillators: (a) nearest-neighbor coupling $l = 1$, see Eq. (4.1), (b) second nearest-neighbor coupling $l = 2$, (c) $l = 3$. Networks in (d)–(f) are described by Eq. (2.1), where (d): $K_1 = K_3 = a$, $K_{-1} = K_{-3} = b$, and $K_2 = K_{-2} = 0$; (e): $K_1 = a_1 \neq K_2 = a_2$ and $K_{-1} = b_1 \neq K_{-2} = b_2$; (f): arbitrary K_j , $j = 0, \dots, 6$. Different colors of arrows denote different coupling strengths.

By introducing new variables

$$\varphi_i = \theta_1 - \theta_{i+1}, \quad i = 1, \dots, N - 1, \quad (2.3)$$

we reduce (2.1) to the system in phase differences

$$\dot{\varphi}_i = \Delta_i + \sum_{j=1}^{N-1} K_j (g(\varphi_j) - g(\varphi_{i+j} - \varphi_i)), \quad i = 1, \dots, N - 1, \quad (2.4)$$

where $\Delta_i = \omega_1 - \omega_{i+1}$, the subscripts are considered modulo N , and $\varphi_0 = 0$. We remark that the original system (2.1) possesses a S^1 phase shift symmetry

$$\theta_i \rightarrow \theta_i + \text{const}$$

that allows to reduce it to the phase differences (2.4) where the reduced system has one less variables and does not have the S^1 symmetry.

In the paper we mainly consider the case of identical oscillators $\Delta_i = 0$, except for Sec. 7. Section 5 investigates examples of low-dimensional systems where $K_j = a$, $K_{-j} = b$, $j = 1, \dots, l$, $l < N/2$ (see Fig. 2.1(a)–(c)), and the coupling function $g(x) = -\sin(x - \alpha)$. In the case of identical oscillators we therefore deal with only two bifurcation parameters b and α , while we can fix $a = 1$.

3 Synchronous solution and rotating waves

In the system of identical oscillators, the synchronous state exists where $\theta_i(t) = \theta_j(t)$ for all i, j and t . In the system for phase differences (2.4) this solution corresponds to the fixed point $\varphi_i = 0$, $i = 1, \dots, N - 1$. In fact, the reduced system (2.4) can have many different fixed points depending on the form of coupling function $g(x)$, however, some of them arise as a result of rotation symmetry of the network. Note that for identical oscillators the circulant structure of the coupling matrix induces an equivariance of the system with respect to the cyclic group Z_N acting by

$$\gamma : (\theta_1, \theta_2, \dots, \theta_N) \mapsto (\theta_N, \theta_1, \dots, \theta_{N-1}).$$

For the reduced system (2.4) this symmetry is given as

$$\tilde{\gamma} : (\varphi_1, \varphi_2, \dots, \varphi_{N-1}) \mapsto (-\varphi_{N-1}, \varphi_1 - \varphi_{N-1}, \dots, \varphi_{N-2} - \varphi_{N-1}).$$

One can check that solutions of (2.1) of the form

$$\left(\theta(t), \theta(t) - \frac{2\pi k}{N}, \dots, \theta(t) - \frac{(N-1)2\pi k}{N} \right), \quad (3.1)$$

$k = 0, \dots, N - 1$ are invariant under the symmetry action γ for arbitrary coupling function $g(x)$. Eq. (3.1) represents *rotating wave* solutions with wave number k , where each oscillator is phase-shifted by $2\pi k/N$ with respect to the neighboring one. The corresponding solutions of the reduced system (2.4) are equilibria

$$\mathcal{M}_k = \left(\frac{2k\pi}{N}, \frac{4k\pi}{N}, \dots, \frac{2(N-1)k\pi}{N} \right). \quad (3.2)$$

The synchronous solution is therefore the rotating wave \mathcal{M}_0 with zero wave number. By substituting (3.2) into (2.4) one can see that the rotating waves with any wave number k exist for any choice of the coupling function g .

Proposition 1. *For any coupling function¹ g , system of coupled identical phase oscillators (2.1) possesses rotating wave solutions (3.1) with all possible wave numbers k . The corresponding solutions of the system in phase differences (2.4) are the equilibria (3.2).*

We note that system (2.4) can have other equilibria in addition to \mathcal{M}_k . Let us first point out the relationship between the system (2.1) and the corresponding system in phase differences (2.4). The following proposition shows that the Jacobian matrices of these two systems evaluated at the corresponding points share the same set of eigenvalues except of the trivial one, which is induced by the phase-shift symmetry of the original system (2.1).

¹Here and hereafter, we assume that $g(\cdot)$ is sufficiently smooth to guarantee the global existence of the solution, but do not mention explicitly.

Proposition 2. *Let A and B the Jacobi matrices of systems (2.1) and (2.4), respectively, that are evaluated at corresponding points $(\theta_1, \dots, \theta_N)$ and $(\varphi_1, \dots, \varphi_{N-1})$, $\varphi_i = \theta_1 - \theta_{i+1}$ ($i = 1, \dots, N-1$). Then the following relation holds*

$$\det(A - \lambda I_N) = -\lambda \det(B - \lambda I_{N-1}),$$

where I_N is $N \times N$ -dimensional identity matrix.

Proof. Let us first rewrite (2.1) and (2.4) in the vector form:

$$\dot{\Theta} = F(\Theta), \quad \Theta = (\theta, \dots, \theta_N), \quad (3.3)$$

and

$$\dot{\Phi} = G(\Phi), \quad \Phi = (\varphi_1, \dots, \varphi_{N-1}). \quad (3.4)$$

We append the first equation $\dot{\theta}_1 = F_1(\theta_1, \dots, \theta_N) = F_1(\theta_1, \theta_1 - \varphi_1, \dots, \theta_1 - \varphi_{N-1})$ of (3.3) to (3.4) and obtain the extended N -dimensional system:

$$\dot{\bar{\Phi}} = \bar{G}(\bar{\Phi}), \quad \bar{\Phi} = (\theta_1, \varphi_1, \dots, \varphi_{N-1}), \quad (3.5)$$

where

$$\bar{\Phi}^T = \begin{pmatrix} \theta_1 \\ \Phi^T \end{pmatrix} = S_N \Theta^T, \quad S_N = \begin{pmatrix} 1 & 0 & \dots & 0 & 0 \\ 1 & -1 & \ddots & \ddots & 0 \\ \vdots & 0 & \ddots & \ddots & \vdots \\ 1 & \vdots & \ddots & -1 & 0 \\ 1 & 0 & \dots & 0 & -1 \end{pmatrix}. \quad (3.6)$$

One can check that $\det(S_N) = (-1)^{N-1}$ and $S_N^{-1} = S_N$. The Jacobian matrices at the corresponding points Θ_0 , Φ_0 , and $\bar{\Phi}_0^T = S_N \Theta_0^T$ are $A = \frac{\partial F}{\partial \Theta}(\Theta_0)$, $B = \frac{\partial G}{\partial \Phi}(\Phi_0)$, and $\bar{B} = \frac{\partial \bar{G}}{\partial \bar{\Phi}}(\bar{\Phi}_0)$. Using the relationship (3.6) we have $\bar{B} = S_N A S_N^{-1}$. It also holds that

$$\bar{B} = \begin{pmatrix} \bar{B}_{11} & \bar{b} \\ \bar{b}^T & B \end{pmatrix},$$

where $\bar{b} = 0$, because the right-hand sides $\bar{G}_2, \dots, \bar{G}_N$ do not depend on θ_1 . Further, the right side of the first equation in (3.5) is $\bar{G}_1(\bar{\varphi}) = \sum_{j=1}^N K_j g(\varphi_j)$, and it is independent of the variable θ_1 , which implies $\bar{B}_{11} = \partial \bar{G}_1 / \partial \theta_1 = 0$. Using the above properties we obtain the necessary result:

$$\begin{aligned} \det(A - \lambda I_N) &= \det(S_N^{-1}(\bar{B} - \lambda I_N)S_N) = \det(\bar{B} - \lambda I_N) \\ &= \det \begin{pmatrix} -\lambda & \bar{b} \\ 0 & B - \lambda I_{N-1} \end{pmatrix} = -\lambda \det(B - \lambda I_{N-1}). \end{aligned} \quad (3.7)$$

□

The additional zero eigenvalue of the matrix A corresponds to the neutral stability of each solution of the original system (3.3) along the eigenvector $v = (1, \dots, 1)$ and appears due to the phase shift symmetry.

The following result establishes the spectrum of the rotating waves \mathcal{M}_k .

Proposition 3. *Eigenvalues of the Jacobi matrix of system (2.1) evaluated at the rotating wave solution \mathcal{M}_k are*

$$\lambda_m(\mathcal{M}_k) = \sum_{j=1}^{N-1} K_j \eta_{kj} \left(1 - e^{i \frac{2mj\pi}{N}}\right), \quad m = 1, \dots, N-1,$$

where $\iota = \sqrt{-1}$ and $\eta_{kj} = g' \left(\frac{2\pi k}{N} j \right)$.

Proof. Let A be the corresponding Jacobi matrix. Direct calculation gives

$$A_{ii}(\mathcal{M}_k) = \sum_{j=1}^N K_{j-i} g'(\mathcal{M}_{k,j-1} - \mathcal{M}_{k,i-1}) = \sum_{j=1}^N K_{j-i} \eta_{k(j-i)} = \sum_{j=1}^N K_j \eta_{kj},$$

$$A_{ij}(\mathcal{M}_k) = -K_{j-i} g'(\mathcal{M}_{k,j-1} - \mathcal{M}_{k,i-1}) = -K_{j-i} \eta_{k(j-i)}, \quad i, j = 1, \dots, N, \quad j \neq i,$$

where $\mathcal{M}_{i,j} = \frac{2\pi i}{N} j$ denotes the component of \mathcal{M}_i . Since $A(\mathcal{M}_k)$ is circulant, it can be presented as a polynomial of the cyclic permutation matrix

$$P_N = \begin{pmatrix} 0 & 1 & 0 & \dots & 0 \\ 0 & 0 & \ddots & \ddots & \vdots \\ \vdots & \vdots & \ddots & \ddots & 0 \\ 0 & 0 & \dots & 0 & 1 \\ 1 & 0 & \dots & 0 & 0 \end{pmatrix}$$

in the following form

$$A(\mathcal{M}_k) = \sum_{j=1}^N K_{j-i} \eta_{k(j-i)} I_N - \sum_{j=1}^N K_{j-i} \eta_{k(j-i)} P_N^{j-i} = \sum_{j=1}^N K_j \eta_{kj} (I_N - P_N^j), \quad (3.8)$$

$k = 0, \dots, N-1$. Eigenvalues of this circulant matrix can be written as

$$\lambda_m(\mathcal{M}_k) = \sum_{j=1}^N K_j \eta_{kj} (1 - \nu_m^j), \quad m = 1, \dots, N, \quad (3.9)$$

where $\nu_m = \exp\left(\frac{2\pi i}{N} m\right)$ are eigenvalues of P_N . Note that equalities $\nu_N^j = \exp\left(\frac{2\pi i}{N} jN\right) = 1$ imply $\lambda_N(\mathcal{M}_k) = 0$. \square

Separating the real and imaginary part, we have also the following expression:

$$\lambda_m(\mathcal{M}_k) = \sum_{j=1}^{N-1} K_j \eta_{kj} \left(1 - \cos\left(\frac{2mj\pi}{N}\right)\right) - \iota \sum_{j=1}^{N-1} K_j \eta_{kj} \sin\left(\frac{2mj\pi}{N}\right). \quad (3.10)$$

This equality implies that the system has $[N/2]$ complex conjugate pairs (the cases when $\text{Im}\lambda = 0$ are also taken into account):

$$\lambda_{N-m}(\mathcal{M}_k) = \lambda_{-m}(\mathcal{M}_k) = \bar{\lambda}_m(\mathcal{M}_k), \quad (3.11)$$

where $[x]$ is the integer part of x , $\bar{\lambda}$ is the complex-conjugate to λ . (3.11) shows that $\text{Im}(\lambda_{N/2}(\mathcal{M}_k)) = 0$ for any \mathcal{M}_k when N is an even number.

The following result follows from Proposition 3 and summarizes the stability properties of \mathcal{M}_k :

Proposition 4. *The following statements hold true:*

– *If the inequality*

$$\operatorname{Re}(\lambda_m(\mathcal{M}_k)) = \sum_{j=1}^{N-1} K_j \eta_{kj} \left(1 - \cos \left(\frac{2mj\pi}{N} \right) \right) < 0$$

holds for all $m = 1, \dots, N-1$, then the rotating wave \mathcal{M}_k is asymptotically stable.

– *If there exists an index $1 \leq m \leq N-1$ such that $\operatorname{Re}(\lambda_m(\mathcal{M}_k)) > 0$ then the rotating wave is unstable.*

– *If there exists an index $1 \leq m \leq N-1$, $m \neq N/2$ such that $\operatorname{Re}(\lambda_m(\mathcal{M}_k)) = 0$ then there exists a pair of complex conjugated eigenvalues*

$$\lambda_{\pm m}(\mathcal{M}_k) = \pm i \Omega_m, \quad \Omega_m = - \sum_{j=1}^{N-1} K_j \eta_{kj} \sin \left(\frac{2mj\pi}{N} \right).$$

Proposition 4 shows that the conditions $\operatorname{Re}(\lambda_m(\mathcal{M}_k)) = 0$ provide stability boundaries for the rotating waves and the synchronous solution $k = 0$. In the case when $\Omega \neq 0$, an Andronov-Hopf bifurcation can take place [24, 48]. We will show in Sec. 4 that for different equilibria the system can have both degenerate and regular Andronov-Hopf bifurcations.

Using the complex conjugacy: $\nu_{-m} = \bar{\nu}_m$ we can rewrite real and imaginary parts of eigenvalues (3.10):

$$\begin{aligned} \operatorname{Re}(\lambda_m(\mathcal{M}_k)) &= \sum_{j=1}^{[(N-1)/2]} (K_j \eta_{kj} + K_{-j} \eta_{-kj}) \left(1 - \cos \left(\frac{2mj\pi}{N} \right) \right) \\ &\quad + \frac{1}{2} ((-1)^N + 1) ((-1)^{m+1} + 1) K_{N/2}, \end{aligned} \quad (3.12)$$

$$\operatorname{Im}(\lambda_m(\mathcal{M}_k)) = - \sum_{j=1}^{[(N-1)/2]} (K_j \eta_{kj} - K_{-j} \eta_{-kj}) \sin \left(\frac{2mj\pi}{N} \right). \quad (3.13)$$

Proposition 4 together with Eq. (3.12) show that it is possible to observe a degenerate bifurcation with up to $[(N-1)/2]$ critical pairs of eigenvalues at the point \mathcal{M}_k .

Remark 5. System (2.4) has other equilibria except for the origin and rotating waves (3.2). For example, it has fixed points $\tilde{\Phi} = (\tilde{\varphi}_1, \dots, \tilde{\varphi}_{N-1})$ with coordinates 0 and π ($\tilde{\varphi}_i \in \{0, \pi\}$). It is easy to check that Jacobian matrix of the system (2.1) at the solution $\tilde{\Theta}$ (corresponding to solutions $\tilde{\Phi}$ of (2.4)) is not circulant. Therefore, the eigenvalues $\lambda_m(\tilde{\Theta})$ can not be described similarly to Eq. (3.9).

4 The model with different forward and backward connections

In this section, we consider the special case when $K_i = a$, $K_{-i} = b$, $i = 1, \dots, l$ and $K_i = 0$ for $l < |i| < N/2$, i.e. each oscillator is connected with identical coupling strength a to its l next neighboring oscillators in the clockwise direction (forward) and with identical coupling strength b to the same number of next neighbors in the counter-clockwise direction (backward). In this case system (2.1) has the form

$$\dot{\theta}_i = \omega_i + a \sum_{j=1}^l g(\theta_i - \theta_{i+j}) + b \sum_{j=N-l}^{N-1} g(\theta_i - \theta_{i+j}), \quad i = 1, \dots, N, \quad (4.1)$$

Further in Sec. 5, low-dimensional examples of such systems will be treated in more detail, especially in the skew symmetric case $a = -b$ leading to the coexistence of Hamiltonian-like and dissipative dynamics. In this section, we state basic stability properties for the rotating waves \mathcal{M}_k for general N . The network is unidirectional when either $a = 0$ or $b = 0$. The schematic diagram in Fig. 2.1 illustrates examples of seven coupled oscillators with (a) $l = 1$, (b) $l = 2$, and (c) $l = 3$ where connections in different directions are marked by arrows of different color.

The system corresponding to (4.1) in phase differences has the form

$$\dot{\varphi}_i = \Delta_i + a \sum_{j=1}^l (g(\varphi_j) - g(\varphi_{i+j} - \varphi_i)) + b \sum_{j=N-l}^{N-1} (g(\varphi_j) - g(\varphi_{i+j} - \varphi_i)), \quad (4.2)$$

$i = 1, \dots, N-1$. In the case of identical oscillators $\omega_i = \omega, i = 1, \dots, N$, without loss of generality we can set $a = 1$ by rescaling the time. In this case, the number of coupling parameters is reduced to just one continuous parameter b , apart from integer parameters N, l , and the coupling function $g(x)$.

By applying the results of Proposition 4 to system (4.2) we obtain the following statement about the stability of rotating waves.

Corollary 6. *The rotating wave solutions $\mathcal{M}_k, k = 0, \dots, N-1$ of system (4.2) undergo a bifurcation, if*

$$\operatorname{Re}(\lambda_m(\mathcal{M}_k)) = \sum_{j=1}^l (a\eta_{kj} + b\eta_{-kj}) \left(1 - \cos\left(\frac{2mj\pi}{N}\right)\right) = 0 \quad (4.3)$$

for some $1 \leq m \leq [(N-1)/2]$. If, additionally, the inequality

$$\Omega := \operatorname{Im}(\lambda_m(\mathcal{M}_k)) = -\sum_{j=1}^l (a\eta_{kj} - b\eta_{-kj}) \sin\left(\frac{2mj\pi}{N}\right) \neq 0 \quad (4.4)$$

holds, then a pair of complex conjugate critical eigenvalues $\lambda_{\pm m} = \pm i\Omega$ appears.

For the case of nearest-neighbor coupling $l = 1$, the condition (4.3) reads

$$\operatorname{Re}(\lambda_m(\mathcal{M}_k)) = (a\eta_k + b\eta_{-k}) \left(1 - \cos\left(\frac{2m\pi}{N}\right)\right) = 0.$$

For $m \neq 0$ (non-synchronous rotating waves), $1 - \cos\left(\frac{2m\pi}{N}\right) > 0$ and the term $a\eta_k + b\eta_{-k}$ is independent of m . Considering also the condition (4.4) in the same way, and recalling the definition of η_k , we have the following statement.

Corollary 7. *The rotating wave solutions \mathcal{M}_k of system (4.2) with nearest-neighbor coupling ($l = 1$) have all eigenvalues purely imaginary if the condition*

$$ag'(2k\pi/N) + bg'(-2k\pi/N) = 0 \quad (4.5)$$

is satisfied. If additionally $g'(2k\pi/N) \neq 0$, then among these eigenvalues there are $[(N-1)/2]$ complex conjugated pairs.

The solution \mathcal{M}_k is asymptotically stable when $ag'(2k\pi/N) + bg'(2k\pi/N) < 0$.

The conditions (4.3) and (4.4) can be simplified at the synchronized solution \mathcal{M}_0 of (4.2) to the following form

$$\operatorname{Re}(\lambda_m(\mathcal{M}_0)) = g'(0)(a+b) \sum_{j=1}^l \left(1 - \cos\left(\frac{2mj\pi}{N}\right)\right) = 0, \quad m = 1, \dots, N-1, \quad (4.6)$$

$$\operatorname{Im}(\lambda_m(\mathcal{M}_0)) = -g'(0)(a-b) \sum_{j=1}^l \sin\left(\frac{2mj\pi}{N}\right) \neq 0. \quad (4.7)$$

The last multiplier on the right hand side of (4.6) is always positive and the last multiplier on the right hand side of (4.7) is nonzero because $m \neq 0, j \neq 0$. For the bifurcation of the synchronous solution we obtain the following conditions.

Corollary 8. *The synchronous solution \mathcal{M}_0 of system (4.2) with nearest-neighbor coupling ($l = 1$) has all eigenvalues purely imaginary if the condition*

$$a = -b \neq 0 \quad \text{or} \quad g'(0) = 0. \quad (4.8)$$

is satisfied. In the case $g'(0) = 0$, all eigenvalues are zero.

The solution \mathcal{M}_0 is asymptotically stable when $ag'(0) + bg'(0) < 0$.

An example, when all eigenvalues are zero is the Kuramoto-Sakaguchi [50] coupling function $g(x) = -\sin(x - \alpha)$ for $\alpha = \pm\pi/2$, there a degenerate transcritical bifurcation occurs, since $g'(0) = -\cos(0 - \alpha) = 0$.

In the case $a = b$ when the coupling is symmetric, the condition (4.3) reduces to

$$\sum_{j=1}^l (\eta_{kj} + \eta_{-kj}) \left(1 - \cos\left(\frac{2mj\pi}{N}\right)\right) = 0. \quad (4.9)$$

In particular, the condition holds for all k , when the derivative of the coupling function is odd $g'(x) = -g'(-x)$. We have the following statements.

Corollary 9. *Let $a = b$ in (4.2) and the coupling function is even $g(x) = g(-x)$. Then the spectrum of all rotating wave solutions \mathcal{M}_k is critical, i.e. $\operatorname{Re}(\lambda_m(\mathcal{M}_k)) = 0$ for all $m = 1, \dots, N-1$ and $k = 0, \dots, N-1$.*

Corollary 10. *Let $a = -b$ in (4.2) and the coupling function is odd $g(x) = -g(-x)$. Then the spectrum of all rotating wave solutions \mathcal{M}_k is critical, i.e. $\operatorname{Re}(\lambda_m(\mathcal{M}_k)) = 0$ for all $m = 1, \dots, N-1$ and $k = 0, \dots, N-1$.*

5 Bifurcation properties in low-dimensional systems

In this section we study in detail the low-dimensional system (4.1)–(4.2) with specific coupling functions. Mostly, we consider a coupling function of Kuramoto-Sakaguchi type [50]

$$g(x) = -\sin(x - \alpha) \quad (5.1)$$

with a phase shift parameter α .

We note that in the case $a = b$ the system (4.2) has the dihedral symmetry D_N . The system (4.2) with Kuramoto-Sakaguchi coupling (5.1) has additional symmetries Γ_1 , Γ_2 , and Γ_3 that are given by the actions:

$$\begin{aligned}\gamma_1 &: (\varphi_1, \dots, \varphi_{N-1}, a, b, \alpha, t) \mapsto (\varphi_1, \dots, \varphi_{N-1}, -a, -b, \alpha, -t), \\ \gamma_2 &: (\varphi_1, \dots, \varphi_{N-1}, a, b, \alpha, t) \mapsto (-\varphi_1, \dots, -\varphi_{N-1}, a, b, -\alpha, -t), \\ \gamma_3 &: (\varphi_1, \dots, \varphi_{N-1}, a, b, \alpha, t) \mapsto (\varphi_1, \dots, \varphi_{N-1}, a, b, \alpha + \pi, -t).\end{aligned}\quad (5.2)$$

For $b = -a$, the system has also the time-reversal symmetry \mathcal{R}

$$\mathcal{R}: (\varphi_1, \dots, \varphi_{N-1}t) \mapsto (\varphi_{N-1}, \dots, \varphi_1, -t), \quad (5.3)$$

which plays an important role for the coexistence of Hamiltonian-like and dissipative dynamics, as it will be discussed in the following.

5.1 Three coupled oscillators

“In this section, we describe the phase space of the system of $N = 3$ identical oscillators with Kuramoto-Sakaguchi coupling function (5.1) written in phase differences (2.4):

$$\begin{aligned}\dot{\varphi}_1 &= -\sin(\varphi_1 - \alpha) - b \sin(\varphi_2 - \alpha) - b \sin(\varphi_1 + \alpha) - \sin(\varphi_1 - \varphi_2 + \alpha), \\ \dot{\varphi}_2 &= -\sin(\varphi_1 - \alpha) - b \sin(\varphi_2 - \alpha) - \sin(\varphi_2 + \alpha) - b \sin(\varphi_2 - \varphi_1 + \alpha).\end{aligned}\quad (5.4)$$

Note that we set the coupling parameter $a = 1$ without loss of generality. In this $N = 3$ case the system is globally coupled (all-to-all). System (5.4) possesses two parameters b and α . The bifurcation diagram with respect to these parameters is shown in Fig. 5.1, and the typical phase portraits for different parameters are shown in Fig. 5.2. In the following, we describe the dynamical properties of the system in details. An important conclusion about the coexistence of Hamiltonian-like and dissipative dynamics will be given in Proposition 11.

Symmetries and fixed points. The Z_3 symmetry in system (5.4) is generated by the action

$$\gamma_{Z_3}: (\varphi_1, \varphi_2) \mapsto (-\varphi_2, \varphi_1 - \varphi_2).$$

The origin $\mathcal{M}_0 = (0, 0)$ and the two rotating wave points $\mathcal{M}_1 = (2\pi/3, 4\pi/3)$, $\mathcal{M}_2 = (4\pi/3, 2\pi/3)$ are invariant under the action γ_{Z_3} . While the locations of these points do not depend on parameters, their stability does. In addition to the \mathcal{M}_k , the system has three Z_3 -symmetric saddles. For $\alpha = 0$, the coordinates of these saddles are $(0, \pi)$, $(\pi, 0)$, and (π, π) , see Fig. 5.2(a), and they change with parameters. The saddles exist for all parameter values except for $\alpha = \pm\pi/2$. Simultaneous connections of stable and unstable one-dimensional manifolds of the three saddles create Z_3 -heteroclinic cycles for some parameter values, see Figs. 5.2(c), (f), (g), and (j).

Bifurcations of fixed points, see Fig. 5.1(a). As follows from Corollary 7 and condition (4.5), the Andronov-Hopf bifurcation lines for the points \mathcal{M}_k are given by the expressions

$$H_k = \left\{ (\alpha, b) : b = -\frac{\cos(2k\pi/3 - \alpha)}{\cos(2k\pi/3 + \alpha)} \right\}, \quad k = 0, 1, 2.$$

In particular, the corresponding bifurcation line for the origin \mathcal{M}_0 is $b = -1 = -a$.

Z_3 -symmetric transcritical bifurcations of the origin occur on the bifurcation lines $\alpha = \pm\pi/2$, where the second condition of (4.8) holds: $g'(0) = 0$. In this case, three symmetric saddle points (Fig. 5.2(a), (b)) approach the origin simultaneously and create a degenerate saddle at the bifurcation moment (Fig. 5.2(d), (k)). Then the saddles pass the origin changing its stability.

Two heteroclinic bifurcation lines HC are very close to the Andronov-Hopf lines H_1 and H_2 of \mathcal{M}_1 and \mathcal{M}_2 , respectively. HC and H lines intersect at the points $(\alpha, b) = (0, -1)$, $(\pm\pi/2, 1)$, $(\pm\pi/2, -1)$ and at the point where coordinate b is close to -0.4 . The global HC bifurcation consists of three symmetric saddle connections and it creates stable (Fig. 5.2(g)) or unstable (Fig. 5.2(f)) heteroclinic cycles. This bifurcation leads to the appearance of a limit cycle with the same stability as the heteroclinic cycle (Fig. 5.2(i), (d)). As a result, limit cycles appear at the H bifurcation and disappear in HC bifurcation (or vice versa). The third symmetric HC bifurcation line coincides with the H_0 line $b = -1$.

The system (2.4) is conservative at the codimension-two bifurcation points $(\alpha, b) = (0, -1)$ (Fig. 5.2(c)) and $(\alpha, b) = (\pm\pi, -1)$. There, it has the first integral

$$I(\varphi_1, \varphi_2) = \cos \varphi_1 + \cos \varphi_2 + \cos(\varphi_1 - \varphi_2).$$

The system is also conservative when $(\alpha, b) = (\pi/2, 1)$ (Fig. 5.2(d)). A similar first integral exist also for more general cases. The system (2.4) for the phases of $N = 3$ coupled oscillators with $K_2 = -K_1$, $K_0 = 0$ and $g(\varphi) = -g(-\varphi)$ has the first integral

$$I(\varphi_1, \varphi_2) = h(\varphi_1) + h(\varphi_2) + h(\varphi_1 - \varphi_2),$$

where $h'(\varphi) = g(\varphi)$.

The regions where the origin is stable consist of two parts: 1) $b > -1$, $\alpha \in (-\pi/2, \pi/2)$ and 2) $b < -1$, $\alpha \in (\pi/2, 3\pi/2)$ (gray color in Fig. 5.1(a)). The regions of the stability of \mathcal{M}_k , $k = 1, 2$, are located between two neighboring H_i lines and it has width π along the α -axis. In particular, the stability region for \mathcal{M}_1 is located between two (blue) bifurcation lines H_1 in Fig. 5.1(a) and it satisfies the inequalities

$$\arctan\left(\frac{1+b}{\sqrt{3}(1-b)}\right) + 2n\pi < \alpha < \arctan\left(\frac{1+b}{\sqrt{3}(1-b)}\right) + (2n+1)\pi, \quad n \in \mathbb{Z}.$$

The case $b = -1$ (α arbitrary) is especially interesting for us. In this case, the system possesses the time-reversal symmetry \mathcal{R} presented by the action (5.3)

$$\mathcal{R} : (\varphi_1, \varphi_2, \alpha, t) \mapsto (\varphi_2, \varphi_1, \alpha, -t).$$

The line $\text{Fix } \mathcal{R} : \{(\varphi_1, \varphi_2), \varphi_1 = \varphi_2\}$ is fixed under this symmetry. The superposition of Z_3 and \mathcal{R} gives two other reversible symmetries with the corresponding fixed subspaces $\varphi_1 = 0$ and $\varphi_2 = 0$.

The system for $b = -1$ has Hamiltonian-like and dissipative regions that coexist in the phase space, see Fig. 5.2(j). The following proposition rigorously states that the phase portrait shown in Fig. 5.2(j) holds qualitatively for almost all values of the parameter α when $b = -1$.

Proposition 11. *For $b = -1$ and $\alpha \notin \{0, \pm\pi/2, \pi\}$, system (5.4) possesses the following dynamics in the phase space:*

(A) *Hamiltonian-like region: there exists a region in the phase space, which contains the origin \mathcal{M}_0 and which is foliated by a one-parametric family of periodic orbits. This region is bounded by a Z_3 -invariant heteroclinic cycle consisting of three saddle points and connecting orbits between them. The*

corresponding saddle points belong to the fixed subspace of the reversibility symmetry $\text{Fix } \mathcal{R}$ or one of its symmetry images under the action of \mathbb{Z}_3 .

(B) *Dissipative region:* The points \mathcal{M}_1 and \mathcal{M}_2 are sink and source, respectively. That is, there exists neighborhoods of the points \mathcal{M}_1 (resp. \mathcal{M}_2), such that all orbits starting from this neighborhoods are asymptotically attracted to \mathcal{M}_1 (resp. repelled from \mathcal{M}_2).

Proof. (A) According to the Corollary 7, under the conditions of the proposition, the origin has the complex conjugated pair of eigenvalues $\pm i\Omega_1 = \pm i\sqrt{3}\cos\alpha \neq 0$. The Lyapunov center theorem for time-reversible systems [23, Theorem 1.1] implies that the system has a one-parameter family $\Phi_\sigma(t)$ of periodic solutions with periods near $2\pi/\Omega_1$ where $\Phi_0(t) = \mathcal{M}_0$ and the parameter σ varies along $\text{Fix } \mathcal{R}$. This shows that a neighborhood of \mathcal{M}_0 is foliated by periodic orbits.

Let us now show that the maximal region \mathcal{D}_0 containing the set of neutral periodic orbits is bounded by the heteroclinic cycle mentioned in the Proposition. It is known that the boundary of an invariant region is flow-invariant. For our two-dimensional system, three types of invariant sets are possible: a limit cycle, a homoclinic cycle, or a heteroclinic cycle. A limit cycle is impossible because it must be neutral from the inside (it borders neutral periodic orbits), and it is neutral from the outside as well, since any trajectory in its small neighborhood intersects $\text{Fix } \mathcal{R}$ twice and is, therefore, periodic. Hence the assumed bounding periodic orbit is neutral and is an internal with respect to \mathcal{D}_0 . A homoclinic cycle cannot be a border of \mathcal{D}_0 , since, according to \mathbb{Z}_3 symmetry, there are three such homoclinic loops that are connected to three different saddles S_i and contain the same neutral fixed point \mathcal{M}_0 . Hence these homoclinic orbits must intersect each other leading to a contradiction. Therefore, a \mathbb{Z}_3 -symmetric heteroclinic cycle is the only possible border for \mathcal{D}_0 . More specifically, it consists of three saddles $S_1(\tilde{\varphi}, \tilde{\varphi}) \in \text{Fix } \mathcal{R}_1$, $S_2(-\tilde{\varphi}, 0) \in \text{Fix } \mathcal{R}_2$, $S_3(0, -\tilde{\varphi}) \in \text{Fix } \mathcal{R}_3$, where $\tilde{\varphi} = \pi - 2\alpha$, $\text{Fix } \mathcal{R}_i = \tilde{\gamma}_{\mathbb{Z}_3}^{i-1} \text{Fix } \mathcal{R}$, $i = 1, 2, 3$, and of three one-dimensional invariant manifolds of these saddles. The region \mathcal{D}_0 has a maximal area when $\alpha = 0$ or $\alpha = \pi$ and it occupies just 3/4 of the phase space \mathbb{T}^2 (Fig. 5.2(c)). Increasing of the parameter $|\alpha|$ from 0 to $\pi/2$ (decreasing $|\alpha|$ from π to $\pi/2$) leads to a symmetric motion of S_i to the origin along $\text{Fix } \mathcal{R}_i$ ($\tilde{\varphi}$ changes from π to 0) that implies further shrinking of the heteroclinic cycle and \mathcal{D}_0 to the origin. Three saddles reach \mathcal{M}_0 when $\alpha = \pm\pi/2$ and they form a degenerate saddle at the bifurcation moment (Fig. 5.2(l)).

(B) For the given parameter values, \mathcal{M}_1 is a sink (with eigenvalues $\lambda_{1,2}(\mathcal{M}_1) = -\frac{3\sqrt{3}}{2}\sin\alpha \pm i\frac{\sqrt{3}}{2}\cos\alpha$) and \mathcal{M}_2 is a source. \square

Our numerical observations (using numerical integration, software AUTO [19], as well as DS-Tool [5]) indicate that the dissipative region extends to $\mathbb{T}^2 \setminus \mathcal{D}_0$.

We will show in further sections that the above described phenomenon of the coexistence of Hamiltonian-like and dissipative dynamics is typical for system (2.4) with an arbitrary number of oscillators and an arbitrary periodic function $g(x)$, when the coupling matrix K is skew symmetric. The case $b = -1 = -a$ is a particular example of skew-symmetric coupling.

We note that system (5.4) also has another time-reversal symmetry \mathcal{R}' given by the action $\mathcal{R}' : (\varphi_1, \varphi_2, t) \mapsto (-\varphi_2, -\varphi_1, -t)$ at the codimension-two point $(\alpha, b) = (0, -1)$ (Figs. 5.2(c) and (d) correspondingly). The fixed subspace of \mathcal{R}' is $\text{Fix } \mathcal{R}' = \{(\varphi_1, -\varphi_1), \varphi_1 \in \mathbb{T}^1\}$, and it is also flow-invariant. A further time-reversal symmetry $\mathcal{R}'' : (\varphi_1, \varphi_2, t) \mapsto (-\varphi_1, -\varphi_2, -t)$ exists when $\alpha = \pm\pi/2$ (Figs. 5.2(d), (k), and (l)). $\text{Fix } \mathcal{R}''$ in this situation consists of only two points $(0, 0)$ and (π, π) in contrast to the previous case where $\text{Fix } \mathcal{R}'$ is a one-dimensional line. We note that the symmetry \mathcal{R}'' exists for the general equation (2.4) with arbitrary even coupling function $g(x)$ and for an arbitrary number of oscillators N .

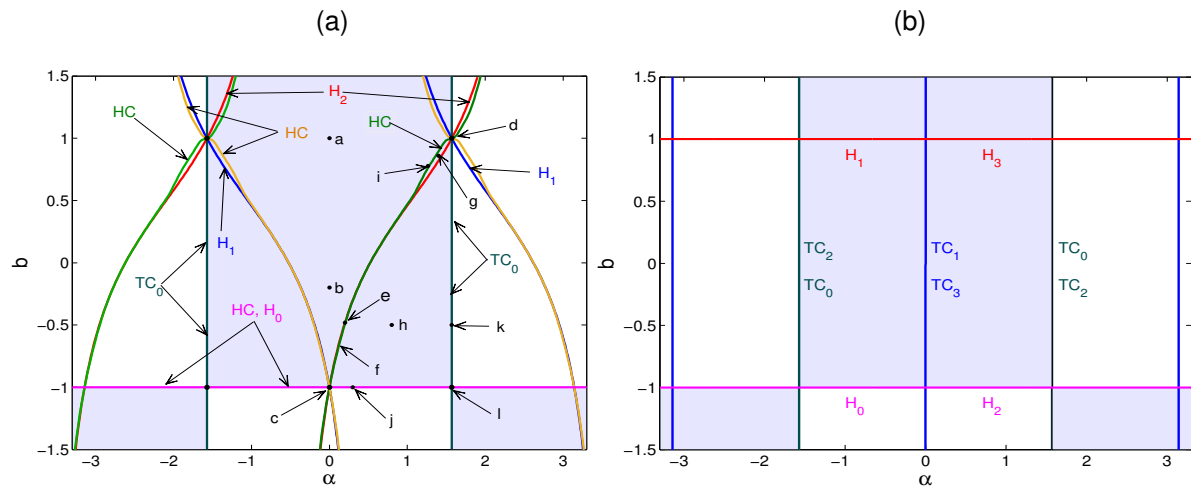


Figure 5.1: Bifurcation diagrams in (α, b) bifurcation plane for three (a) and four (b) coupled oscillators. H_k : line of the Andronov-Hopf bifurcation of \mathcal{M}_k ; TC_k : transcritical bifurcation of \mathcal{M}_k ; HC : heteroclinic (saddle-connection). Lines HC and H_2 (H_1) are located very close to each other, they intersect when $b \approx -0.4$ and partially merge in the figure. The Points $a-l$ indicate parameter values, for which corresponding qualitatively different phase portraits are shown in Fig. 5.2. g and f indicate upper and lower parts of the same HC line; i and e indicate upper and lower regions between H_2 and HC ; $c(0, 1)$, $d(\pi/2, 1)$, $l(\pi/2, -1)$ are codimension-2 bifurcation points; j belongs to H_0 between c and l ; k belongs to TS_0 between d and l . Shaded regions show stability regions of the synchronous solution.

5.2 Four coupled oscillators

System (4.2) of $N = 4$ identical oscillators is three-dimensional for the phase differences $(\varphi_1, \varphi_2, \varphi_3)$:

$$\dot{\varphi}_i = g(\varphi_1) - g(\varphi_{i+1} - \varphi_i) + b(g(\varphi_3) - g(\varphi_{i+3} - \varphi_i)), \quad i = 1, 2, 3, \quad (5.5)$$

where $g(x) = -\sin(x - \alpha)$. Here we also set $a = 1$ without loss of generality. Apart from the synchronous solution \mathcal{M}_0 at the origin, system (5.5) possesses the equilibria $\mathcal{M}_1 = (\pi/2, \pi, 3\pi/2)$, $\mathcal{M}_2 = (\pi, 0, \pi)$, and $\mathcal{M}_3 = (3\pi/2, \pi, \pi/2)$.

The bifurcation diagram in the parameter plane (α, b) for $N = 4$ is shown in Fig. 5.1(b), where Andronov-Hopf (H) and transcritical (TC) bifurcation lines of the rotating waves are plotted. The stability region for the origin is the same as in the case of three oscillators. The stability region of the point \mathcal{M}_2 coincides with the instability region of the origin. Stability regions of two points \mathcal{M}_1 and \mathcal{M}_3 are also complementary to each other. These regions are bounded by the lines $\alpha = 0$, $\alpha = \pi$, and $b = 1$. The system is conservative at the codimension-two points $(\alpha, b) = (0, -1)$ and $(\alpha, b) = (\pi, -1)$ with the first integral $I_1(\varphi_1, \varphi_2, \varphi_3) = \varphi_1 - \varphi_2 + \varphi_3$. In these cases, the whole phase space \mathbb{T}^3 is filled with a continuous set of non-isolated periodic orbits that are located within the parallel planes $\varphi_1 - \varphi_2 + \varphi_3 = \text{constant}$. The plane $\varphi_1 - \varphi_2 + \varphi_3 = \pi$ consists of degenerate saddle points. The system also has another first integral $I_2(\varphi_1, \varphi_2, \varphi_3) = \cos(\varphi_1) + \cos(\varphi_1 - \varphi_2) + \cos(\varphi_2 - \varphi_3) + \cos(\varphi_3)$. Therefore, the periodic orbits in the mentioned planes are described by expressions $\cos(\varphi_1) + \cos(\varphi_1 - \varphi_2) + \cos(\varphi_1 - c_1) + \cos(\varphi_1 - \varphi_2 - c_1) = c_2$, where the constant c_1 corresponds to the choice of a certain plane and the constant c_2 to the choice of a certain periodic curve in this plane.

The last situation can be generalized for arbitrary coupling function $g(\varphi)$ with two the first integrals $I_1(\varphi_1, \varphi_2, \varphi_3) = \varphi_1 - \varphi_2 + \varphi_3$ and $I_2(\varphi_1, \varphi_2, \varphi_3) = h(\varphi_1) + h(\varphi_1 - \varphi_2) + h(\varphi_2 - \varphi_3) + h(\varphi_3)$,

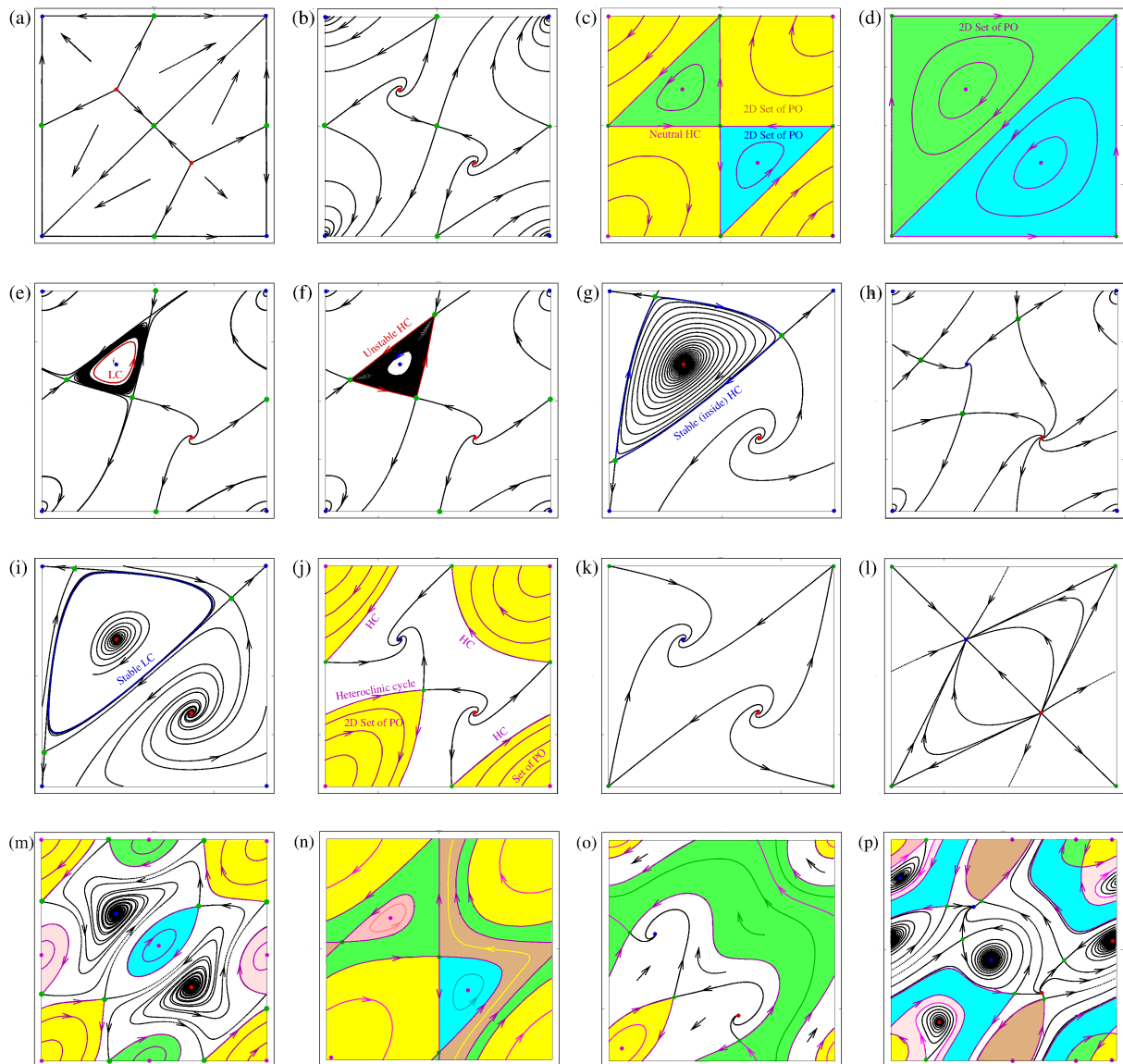


Figure 5.2: Phase portraits for different parameter values for $N = 3$ coupled oscillators. Phase portraits in (a)–(l) correspond to system (5.4) and parameters from the points a to l in Fig. 5.1(a). Phase portraits (m), (o), and (p) correspond to the coupling function (9.1) with additional second harmonic term. (n)–(p): phase portraits for different natural frequencies of the oscillators. Colored areas indicate Hamiltonian-like regions in the phase space that are filled with neutrally stable limit cycles. Colors for fixed points indicate: red — source, blue — sink, green — saddle, magenta — center, dark green — degenerate saddle. Stable limit cycles are shown in blue, unstable in red.

where $h'(\varphi) = g(\varphi)$.

The case of skew-symmetric coupling $b = -1$ leads to the emergence of coexisting Hamiltonian-like and dissipative dynamics as in the case $N = 3$. The following proposition describes it in more detail. As in the previous case, the conservative dynamics appears due to the time-reversibility (5.3).

Proposition 12. *For $b = -1$ and $\alpha \notin \{0, \pm\pi/2, \pm\pi\}$ system (5.5) possesses the following dynamics in the phase space:*

(A) *Hamiltonian-like region: there exist neighborhoods of the equilibria \mathcal{M}_0 and \mathcal{M}_2 , which are foliated by two-parametric families of periodic orbits.*

(B) *Dissipative region: The equilibria \mathcal{M}_1 and \mathcal{M}_3 are sink and source, respectively. That is, there exist neighborhoods of the points \mathcal{M}_1 (resp. \mathcal{M}_3), such that all orbits starting from this neighborhood are asymptotically attracted to \mathcal{M}_1 (resp. repelled from \mathcal{M}_3).*

Proof. (A) The time-reversal symmetry \mathcal{R} has the 2-dimensional fixed subspace

$$\text{Fix } \mathcal{R} : \{(\varphi_1, \varphi_2, \varphi_3) : \varphi_1 = \varphi_3\}.$$

According to (3.9), the eigenvalues of the origin are $\lambda_{1,3}(\mathcal{M}_0) = \pm i\Omega_1 = \pm i2 \cos(\alpha)$ and $\lambda_2 = 0$. It follows from [23, Theorem 2.2] that there exists a 2-parameter family of periodic solutions in the neighborhood of \mathcal{M}_0 with periods near $2\pi/\Omega_1$. Hence, there exists an invariant region \mathcal{D}_0 around the origin that is foliated with non-isolated limit cycles. The fixed point \mathcal{M}_2 belongs also to $\text{Fix } \mathcal{R}$ and it has properties similar to \mathcal{M}_0 . Hence, \mathcal{M}_2 also possesses a neighborhood \mathcal{D}'_0 , which is foliated with non-isolated limit cycles as well.

(B) Using (3.9) one can check that the fixed point \mathcal{M}_1 is a sink or a source when $b = -1$ and $\alpha \notin \{0, \pm\pi\}$. The reversibility \mathcal{R} implies that the point \mathcal{M}_3 symmetric to \mathcal{M}_1 possesses stability properties opposite to \mathcal{M}_1 . Finally we note again that the Hamiltonian-like regions \mathcal{D}_0 and \mathcal{D}'_0 shrink to points when $|\alpha|$ approach $\pi/2$. \square

The following observations provide more details and complete the global picture of the dynamics in the phase space for $b = -1$, they are also summarized in Fig. 5.3. We note that the superposition of Z_4 and \mathcal{R} gives another time-reversal symmetry \mathcal{R}' with $\text{Fix } \mathcal{R}' : \{(\varphi_1, \varphi_2, \varphi_3) : \varphi_2 = 0\}$. The intersection of the planes $\text{Fix } \mathcal{R}$, $\text{Fix } \mathcal{R}'$ gives the 1D flow-invariant subspace $V_0 = \text{Fix } \mathcal{R} \cap \text{Fix } \mathcal{R}' = \{(\varphi, 0, \varphi), \varphi \in \mathbb{T}^1\} = \text{span } v$, where $v = (1, 0, 1)$ is an eigenvector corresponding to the eigenvalue $\lambda_2 = 0$ of the equilibrium \mathcal{M}_0 . It is easy to check that the whole line V_0 is filled with equilibria. The equilibrium \mathcal{M}_2 belongs also to subspace V_0 . The equilibria in $V_0 \cap (\mathcal{D}_0 \cup \mathcal{D}'_0)$ are neutral in the directions transverse to V_0 and they are saddles otherwise, outside of the conservative regions. Each periodic trajectory rotates around V_0 and it has two intersections with invariant plane $\text{Fix } \mathcal{R}$ at the points $(\bar{\varphi}_1, \bar{\varphi}_2, \bar{\varphi}_1)$, $(\bar{\varphi}_1 - \bar{\varphi}_2, -\bar{\varphi}_1, \bar{\varphi}_1 - \bar{\varphi}_2)$ and two corresponding intersections with $\text{Fix } \mathcal{R}'$ at the points $(-\bar{\varphi}_1, 0, \bar{\varphi}_2 - \bar{\varphi}_1)$, $(\bar{\varphi}_2 - \bar{\varphi}_1, 0, -\bar{\varphi}_1)$. One can check that the plane $\text{Fix } \mathcal{R}$ contains two lines of non-isolated fixed points $\varphi_2 = 2(\varphi_1 + \alpha) \pm \pi$ (or, equivalently, this is one line in \mathbb{T}^2 with rotation number 1:2). Each fixed point of the line is a degenerate saddle, it is neutral along the line and it has attractive and repulsive 1D invariant manifolds in directions transversal to the line. According to the rotational symmetry, another invariant plane $\text{Fix } \mathcal{R}'$ has also one-parametric lines of degenerate saddles defined by the expression $\varphi_3 = -\varphi_1 + 2\alpha \pm \pi$. Fixed points on the intersection of the above mentioned line with V_0 have all zero eigenvalues. There are four such points with coordinates $(\pm\pi \pm \alpha, 0, \pm\pi \pm \alpha)$ that are on the boundary between the conservative and the dissipative parts (Fig. 5.3).

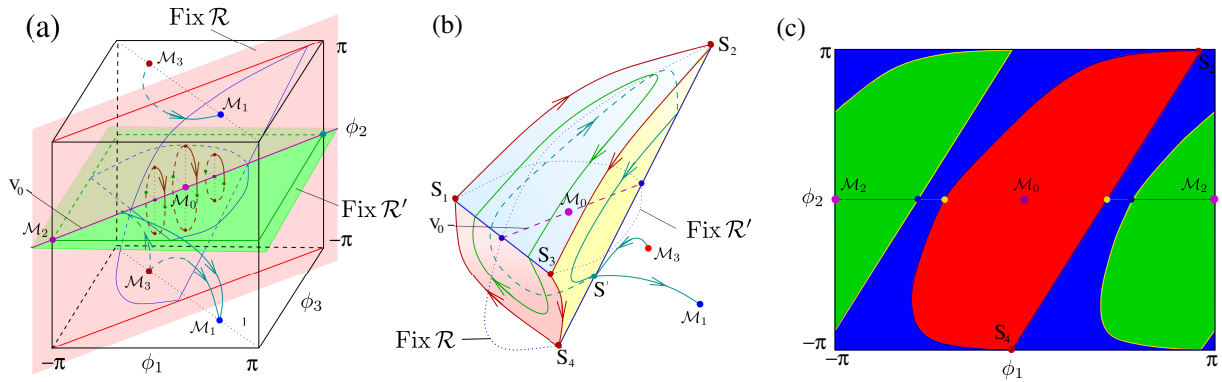


Figure 5.3: (a) Structure of the phase space of the system of four coupled oscillators (5.5) for $b = -a = -1$ and $\alpha \in (0, \pi/2)$. (b) Hamiltonian-like region \mathcal{D} filled by a 2-parametric family of periodic orbits and bounded by a surface of heteroclinic cycles. (c) Fixed subspace for the time-reversibility transformation $\text{Fix } \mathcal{R}$ as a Poincaré section for the system when $\alpha = 0.2$. Blue region indicates the intersection of $\text{Fix } \mathcal{R}$ with the attraction basin of the rotating wave \mathcal{M}_1 (heteroclinic trajectories start at \mathcal{M}_3 , intersect $\text{Fix } \mathcal{R}$ and converge to \mathcal{M}_1). Red and green regions indicate families of non-isolated periodic orbits that intersect $\text{Fix } \mathcal{R}$ transversally in neighborhoods of \mathcal{M}_0 and \mathcal{M}_2 respectively.

The one-parametric family of the invariant 1D manifolds of saddles form a 2D surface (tube), which is the boundary between the Hamiltonian-like region \mathcal{D}_0 (\mathcal{D}'_0) and the dissipative region. The whole separatrix surface consists of heteroclinic cycles that connect two degenerate saddles of the same invariant line. There are also heteroclinic orbits that connect the saddle of the invariant line and the sink \mathcal{M}_1 (or the source \mathcal{M}_3).

5.3 Five coupled oscillators

In the case of five coupled oscillators

$$\dot{\varphi}_i = g(\varphi_1) - g(\varphi_{i+1} - \varphi_i) + b(g(\varphi_3) - g(\varphi_{i+3} - \varphi_i)), \quad i = 1, 2, 3, 4, \quad (5.6)$$

$g(x) = -\sin(x - \alpha)$, the situation is more complicated, since the phase space is 4-dimensional, and we are not able to give a complete description of the phase space structure as in the case of $N \leq 4$. Nevertheless, one can still show the coexistence of dissipative and Hamiltonian-like regions that are densely filled with two-dimensional tori and families of periodic orbits. Figure 5.4(a) illustrates different trajectories belonging to the dissipative domain (heteroclinic orbit shown in red) and Hamiltonian-like (tori in green and magenta, as well as a periodic orbit in blue).

The following proposition holds.

Proposition 13. For $b = -1$ and $\alpha \notin \{0, \pm\pi/2, \pm\pi\}$, system (5.6) possesses the following dynamics in the phase space:

(A) *Hamiltonian-like region:* (i) In a neighborhood of \mathcal{M}_0 there exists a one-parameter family of periodic solutions. (ii) In any neighborhood of \mathcal{M}_0 there exists an analytic 2-dimensional torus, which is invariant with respect to the flow and with respect to the reversibility transformation \mathcal{R} . Moreover, if U_ε is an ε -neighborhood of \mathcal{M}_0 , then the Lebesgue measure of the invariant tori tends to the full measure of the neighborhood U_ε , as $\varepsilon \rightarrow 0$.

(B) *Dissipative region:* For $0 < \alpha < \pi$, the rotating waves $\mathcal{M}_1, \mathcal{M}_2$ are sinks and $\mathcal{M}_3, \mathcal{M}_4$ are sources. For $-\pi < \alpha < 0$, the stability is inverse, i.e. $\mathcal{M}_1, \mathcal{M}_2$ are sources and $\mathcal{M}_3, \mathcal{M}_4$ sinks.

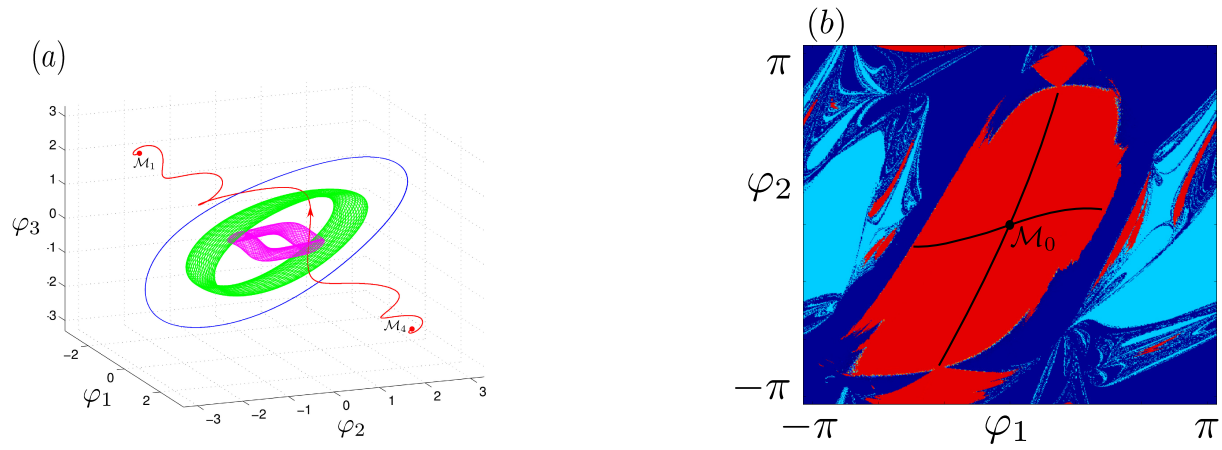


Figure 5.4: (a) Trajectories of (5.6) for $\alpha = 0.2$. Blue trajectory is periodic, green and magenta are quasi-periodic with different amplitude, red trajectory is heteroclinic and it connects the repeller \mathcal{M}_4 with the attracting equilibrium \mathcal{M}_1 . The first three trajectories belong to the Hamiltonian-like part of the system while the last one belongs to the dissipative part. (b) Different domains of the fixed point subspace of the involution \mathcal{R} : red: Hamiltonian-like region, where all Lyapunov exponents are close to zero; light and dark blue: attraction basin of one of the asymptotically stable rotating waves. Black lines correspond to the families of periodic orbits.

The proof follows from the general Proposition 15 in Sec. 6. Roughly speaking, statement (A) is a consequence of the KAM theory for reversible systems [52, 53], and the second part follows from the stability analysis of the rotating wave points. In Fig. 5.4(b) we illustrate numerically the dynamics using the two-dimensional fixed point subspace of the involution \mathcal{R} :

$$\text{Fix } \mathcal{R} = \{(\varphi_1, \varphi_2, \varphi_3, \varphi_4) : \varphi_1 = \varphi_4, \varphi_2 = \varphi_3\}.$$

Figure 5.4(b) shows which part of $\text{Fix } \mathcal{R}$ belong to the Hamiltonian-like region (red domain) and which to the dissipative one (blue domains). In particular the red domain corresponds to the points, which lead to the orbits with all four Lyapunov exponents close to zero (less than 10^{-4} in absolute value). The blue domain belongs to the attraction basin of one of the rotating wave: light-blue to \mathcal{M}_2 and dark-blue to \mathcal{M}_1 . Black lines in Fig. 5.4(b) show the Poincare-sections for the one-parametric families of periodic orbits.

6 Coexistence of Hamiltonian-like and dissipative dynamics in systems of coupled identical oscillators

In this section, we consider system (2.1) with arbitrary number N of coupled identical oscillators. Our main goal is to show that the splitting of the phase space into regions with dissipative and Hamiltonian-like dynamics, which was observed for low-dimensional systems in Sec. 5, remains, provided the coupling is skew-symmetric, i.e. $K_j = -K_{-j}$.

For the skew-symmetric coupling, systems (2.1) and (2.4) can be written as follows

$$\dot{\theta}_i = \omega + \sum_{j=1}^{[(N-1)/2]} K_j (g(\theta_i - \theta_{i+j}) - g(\theta_i - \theta_{i-j})), \quad (6.1)$$

$$\dot{\varphi}_i = \sum_{j=1}^{[(N-1)/2]} K_j (g(\varphi_j) - g(\varphi_{-j}) - g(\varphi_{i+j} - \varphi_i) + g(\varphi_{i-j} - \varphi_i)) \quad (6.2)$$

with $i = 1, \dots, N-1$. Note, that $K_0 = 0$ as well as $K_{N/2} = 0$ when N is even. As it was mentioned, the origin \mathcal{M}_0 and \mathcal{M}_k are equilibria for the system in phase differences (6.2).

Let us firstly show that system (6.2) is time-reversible.

Lemma 14. *System (6.2) has time-reversal symmetry*

$$\mathcal{R} : (\varphi_1, \dots, \varphi_{N-1}, t) \mapsto (\varphi_{N-1}, \dots, \varphi_1, -t). \quad (6.3)$$

Proof. One can check that

$$\begin{aligned} G_i(\mathcal{R}\Phi) &= G_i(\varphi_{N-1}, \dots, \varphi_1) \\ &= \sum_{j=1}^{[(N-1)/2]} K_j (g(\varphi_{-j}) - g(\varphi_j) - g(\varphi_{-(i+j)} - \varphi_{-i}) + g(\varphi_{-(i-j)} - \varphi_{-i})) \\ &= - \sum_{j=1}^{[(N-1)/2]} K_j (g(\varphi_j) - g(\varphi_{-j}) - g(\varphi_{(-i)+j} - \varphi_{-i}) + g(\varphi_{(-i)-j} - \varphi_{-i})) \\ &= -G_{-i}(\varphi_1, \dots, \varphi_{N-1}) = -G_{N-i}(\Phi) \end{aligned}$$

for any $i = 1, \dots, N-1$. This implies

$$(G_1(\mathcal{R}\Phi), \dots, G_{N-1}(\mathcal{R}\Phi))^T = -\mathcal{R}(G_1(\Phi), \dots, G_{N-1}(\Phi))^T.$$

□

We emphasize that the reversibility property is independent of the coupling function $g(x)$.

The fixed subspace of the involution \mathcal{R} is

$$\text{Fix } \mathcal{R} = \{\Phi \in \mathbb{T}^{N-1} : \mathcal{R}\Phi = \Phi\} = \left\{ \Phi \in \mathbb{T}^{N-1} : \varphi_i = \varphi_{N-i}, 1 \leq i \leq \left\lfloor \frac{N-1}{2} \right\rfloor \right\}.$$

Generically, the dimension of this set is $d(N) := \dim(\text{Fix } \mathcal{R}) = N-1 - [(N-1)/2] = [N/2]$. The subspace $\text{Fix } \mathcal{R}$ can be used for describing the dynamical features of the system, because of the following properties:

- If some orbit intersects $\text{Fix } \mathcal{R}$ at two points, then it is periodic, and it consists of two parts that are mapped into each other by the involution \mathcal{R} .
- Any non-periodic trajectory can intersect $\text{Fix } \mathcal{R}$ only once (in the opposite case this trajectory is periodic).
- If a reversible system has a sink or source equilibrium, then it does not belong to $\text{Fix } \mathcal{R}$.
- If a reversible system has a sink (source) \mathcal{M} , then $\mathcal{R}\mathcal{M}$ is an equilibrium, and it is a source (sink).
- If a trajectory starts from a source and intersects $\text{Fix } \mathcal{R}$, then it tends to a symmetry related sink, and this trajectory is heteroclinic (as in Figs. 5.2, 5.3 and 5.4). Note that the reversibility does not imply

the existence of a trajectory that starts from a source and intersects with $\text{Fix } \mathcal{R}$, i.e. the sink and the related source can be disconnected.

Since all trajectories that intersect $\text{Fix } \mathcal{R}$ two times are time-periodic, it is instructive to consider the intersection of $\text{Fix } \mathcal{R}$ with its evolution under the flow:

$$\mathcal{F}_t(\text{Fix } \mathcal{R}) = \{\Phi(t) : \Phi(0) \in \text{Fix } \mathcal{R}, t \in \mathbb{R}\}.$$

Reversible periodic trajectories appear for all points of the intersection $\text{Fix } \mathcal{R} \cap \mathcal{F}_t(\text{Fix } \mathcal{R})$. Since the dimension of $\mathcal{F}_t(\text{Fix } \mathcal{R})$ is $d_t(N) := \dim(\mathcal{F}_t(\text{Fix } \mathcal{R})) = [N/2] + 1$, according to the transversality theorem, the dimension of the intersection in \mathbb{T}^{N-1} is generically

$$d^*(N) := \dim(\text{Fix } \mathcal{R} \cap \mathcal{F}_t(\text{Fix } \mathcal{R})) = d(N) + d_t(N) - (N - 1) = \begin{cases} 1, & \text{when } N \text{ is odd,} \\ 2, & \text{when } N \text{ is even.} \end{cases}$$

Therefore, we generically expect that system (6.2) possesses one or two-parametric families of periodic orbits, depending on the parity of the phase space dimension. Such families have been already described in the low-dimensional cases in Sec. 5. In particular, for the cases $N = 3$ and $N = 4$, when the phase space of (6.2) is 2 and 3, respectively, the families of periodic orbits occupied open sets of the phase space forming the Hamiltonian-like domains filled with just periodic orbits, see Sec. 5.1 and 5.2. However, already for $N = 5$, when the phase space is four-dimensional, the families of periodic orbits do not occupy an open subset of the phase space, but rather form two-dimensional invariant manifolds, as in Sec. 5.3. As a result, other states appear such as quasiperiodic, as in case $N = 5$ (Sec. 5.3), or chaotic.

For a general system (6.2) of N coupled oscillators, the following proposition holds.

Proposition 15. *For $g'(0) \neq 0$ system (6.2) possesses the following dynamics:*

(A) *Families of periodic orbits in the vicinity of \mathcal{M}_0 : For almost all skew-symmetric couplings K such that $K_j = -K_{-j}$, there exists a one-parameter family of periodic solutions $\Phi_\sigma(t)$ in the neighborhood of \mathcal{M}_0 when N is odd and a two-parameter family $\Phi_{(\sigma_1, \sigma_2)}(t)$ of periodic solutions when N is even, with periods close to $2\pi/\Omega_m$, where $\Omega_m = 2g'(0) \sum_{j=1}^{[(N-1)/2]} K_j \sin\left(\frac{2mj\pi}{N}\right)$.*

(B) *Dense set of invariant tori in the vicinity of \mathcal{M}_0 : Under the non-resonance and non-degeneracy conditions (b1) and (b2), given below, in any neighborhood of \mathcal{M}_0 there exist analytic $[(N-1)/2]$ -dimensional tori with conditionally-periodic motions with incommensurable frequencies close to $\Omega_1, \dots, \Omega_{[(N-1)/2]}$. The tori are invariant with respect to the flow and with respect to the reversibility transformation \mathcal{R} . Moreover, if U_ε is an ε -neighborhood of \mathcal{M}_0 , then the Lebesgue measure of the invariant tori tends to the full measure of the neighborhood U_ε , as $\varepsilon \rightarrow 0$.*

– (b1) *Non-resonance: $(q, \Omega) = \sum_{m=1}^{[(N-1)/2]} q_m \Omega_m \neq 0$ is satisfied for all q with $|q| \leq 2l + 2$ and some $l \in \mathbb{N}$.*

– (b2) *Non-degeneracy: The leading cubic terms (i.e. their imaginary parts) of the normal form are non-degenerate (equiv. to operator Γ in [53]).*

(C) *The statements (A) and (B) hold also for a neighborhood of $\mathcal{M}_{N/2}$ if N is even.*

(D) *Dissipative dynamics: The equilibrium \mathcal{M}_k , $k \neq 0$, is a sink if the condition*

$$\text{Re}(\lambda_m(\mathcal{M}_k)) = \sum_{j=1}^{[(N-1)/2]} K_j (\eta_{kj} - \eta_{-kj}) \left(1 - \cos\left(\frac{2mj\pi}{N}\right)\right) < 0 \quad (6.4)$$

satisfied for all $m = 1, \dots, N - 1$. In this case \mathcal{M}_{-k} is a source.

Proof. (A) The existence of families of periodic orbits can be shown using Lyapunov center theorem for time-reversible systems [63, 23]. Using the skew-symmetry of the matrix K and expression (3.10), the eigenvalues of the synchronous state \mathcal{M}_0 are

$$\begin{aligned} \lambda_m(\mathcal{M}_0) &= g'(0) \sum_{j=1}^{[(N-1)/2]} (K_j + K_{-j}) \left(1 - \cos\left(\frac{2mj\pi}{N}\right)\right) \\ &\quad - ig'(0) \sum_{j=1}^{[(N-1)/2]} (K_j - K_{-j}) \sin\left(\frac{2mj\pi}{N}\right) = \\ &\quad -i2g'(0) \sum_{j=1}^{[(N-1)/2]} K_j \sin\left(\frac{2mj\pi}{N}\right) =: i\Omega_m, \end{aligned} \quad (6.5)$$

for any $m = 1, \dots, N-1$. Hence, $\lambda_{\pm m}(\mathcal{M}_0) = \pm i\Omega_m$, $m = 1, \dots, [(N-1)/2]$, and $\lambda_{N/2}(\mathcal{M}_0) = 0$ if N is even. It is easy to see from (6.5) that the following non-resonance conditions are satisfied for almost all values of K_j for $N \geq 5$, and for all values of K for $N = 3, 4$:

- i) all $i\Omega_m$ are simple eigenvalues of the Jacobi matrix $B(\mathcal{M}_0)$;
- ii) $m\Omega_m$ are not eigenvalues of $B(\mathcal{M}_0)$ for all $n > 1$.

When N is odd, the conditions of [23, Theorem 1.1] are satisfied in the neighborhood of $\mathcal{M}_0 \in \text{Fix } \mathcal{R}$. Therefore, there exists a one-parameter family of periodic solutions $\Phi_\sigma(t)$ of (6.2).

In the case of N even, Theorem 2.1 from [23] is applicable. In order to satisfy the conditions of this theorem, it is necessary to check that \mathcal{R} is the identity transformation on $\ker(B(\mathcal{M}_0))$. Indeed, the eigenvector of the trivial eigenvalue $\lambda_{N/2}(\mathcal{M}_0) = 0$ is $v = (1, 0, 1, 0, \dots, 1, 0, 1)^T$, and $V_0 = \ker(B(\mathcal{M}_0)) = \text{span}(v) = (\varphi, 0, \varphi, 0, \dots, \varphi, 0, \varphi)$, $\varphi \in \mathbb{T}^1$, hence $\dim V_0 = 1$, and one can check that $\mathcal{R}v = v$. Therefore, as follows from [23, Theorem 2.1], there exists a 2-parameter family of periodic orbits for even N in the vicinity of \mathcal{M}_0 . The period of these solutions is close to $2\pi/\Omega_m$.

(B) The existence of dense families of quasiperiodic tori follows from the KAM theory for reversible systems [53, 40, 4, 12, 11, 13, 35]. Under the non-resonance and non-degeneracy conditions (b1) and (b2), the conditions of the Theorem from [53] are satisfied. More specifically, the dimensions of tori are $(N-1)$ for odd N and $(N-2)$ for even N (in notations of [53]: $m = (N-1)/2$, $k = 0$ for odd, and $m = (N-2)$, $k = 1$ for even dimensions).

(C) It is easy to check that the equilibrium $\mathcal{M}_{N/2}$ is neutral because $\eta_{N/2j} - \eta_{-N/2j} = 0$ and, therefore, $\text{Re}(\lambda_m(B(\mathcal{M}_{N/2}))) = 0$ for any m . Since $\mathcal{M}_{N/2} \in \text{Fix } \mathcal{R}$, the same arguments as in (A) and (B) can be applied.

(D) We know that the system has equilibria \mathcal{M}_k independently of system parameters and we can check the stability of these points using Propositions 3–4. In particular, the real parts of the eigenvalues of \mathcal{M}_k , $k \neq 0$, are

$$\text{Re}(\lambda_m(\mathcal{M}_k)) = \sum_{j=1}^{[(N-1)/2]} K_j (\eta_{kj} - \eta_{-kj}) \left(1 - \cos\left(\frac{2mj\pi}{N}\right)\right), \quad (6.6)$$

$m = 1, \dots, N-1$. According to the time-reversal symmetry \mathcal{R} the equilibrium \mathcal{M}_{-k} is a source if \mathcal{M}_k is a sink and vice-versa. \square

Remark 16. The families of periodic orbits fill an open set in the phase space around the origin in the cases $N = 3$ and $N = 4$. The situation is different for higher dimensions. In particular, for $N = 5$, the intersection of the family of periodic orbits with two-dimensional manifold $\text{Fix } \mathcal{R}$ consists

of two one-dimensional curves $P_1(\Phi)$ and $P_2(\Phi)$, see Fig. 5.4. These two curves intersect at the origin: $\mathcal{M}_0 = P_1(\Phi) \cap P_2(\Phi) \in \text{Fix } \mathcal{R}$. Solutions with initial conditions on $P_1(\Phi)$ have the period near $2\pi/\tilde{\omega}_1$, and the solutions starting on $P_2(\Phi)$ have periods near $2\pi/\tilde{\omega}_2$. There are at least two intersections of each periodic solution with $\text{Fix } \mathcal{R}$.

The condition (6.4) is only sufficient, and it can be weakened using the fact that the system can have other attractors/repellers except for \mathcal{M}_k .

Remark 17. The cases when $g(x)$ is odd or even can be special. One can see that condition (6.4) is not satisfied when the function $g(x)$ is odd. Also $\text{Im}(\lambda_m(\mathcal{M}_0)) = 0$, $m = 1, \dots, N-1$, when $g(x)$ is even. This implies that in this situation the origin is a degenerate saddle and the conservative region may shrink to one point.

We note that the superposition of symmetries Z_N and \mathcal{R} implies the existence of $N-1$ other reversal symmetries \mathcal{R}_i , $i = 2, \dots, N$. Hence, there exist $N-1$ hyperplanes $\text{Fix } \mathcal{R}_i = \gamma_{Z_N}^i \text{Fix } \mathcal{R}_1$ that are fixed under the transformations \mathcal{R}_i , $i = 2, \dots, N-1$. All $\text{Fix } \mathcal{R}_i$ intersect in \mathcal{M}_0 if N is odd and they intersect along one-dimensional line $V_0 \in \mathbb{T}^{N-1}$ when N is even. If a periodic orbit intersects only one $\text{Fix } \mathcal{R}_i$ in two points, then there are N Z_N -symmetry related periodic orbits. If a periodic orbit intersects at least two $\text{Fix } \mathcal{R}_i$, then it intersects all of them. As in the considered low-dimensional cases, the Hamiltonian-like dynamics is localized around the origin when N is odd and this dynamics translates along line V_0 when N is even. There are also the second ‘‘island’’ of Hamiltonian-like dynamics in the even-dimensional case around a neutral fixed point $\mathcal{M}_{N/2}$.

7 Nonidentical oscillators

7.1 Divergence-free dynamics

We have shown that system (2.4) is Hamiltonian-like in the whole phase space for three and four oscillators when coupling function $g(x) = -\sin x$ and $a = -b$. The system has N neutral rotating wave points \mathcal{M}_k , saddles, heteroclinic structures, continuous sets of periodic orbits (as shown in Fig. 5.2(c) for three oscillators) and quasi-periodic or chaotic trajectories (for higher dimensions). In such a case, the vector field has zero divergence even for arbitrary frequency differences Δ_i . The following proposition holds.

Proposition 18. (A) *The system (2.4) with arbitrary frequency differences Δ_i , $i = 1, \dots, N-1$, skew-symmetric coupling $K_{-j} = -K_j$ and odd coupling function $g(x)$ is divergence free.*
 (B) *The system (2.4) with arbitrary frequency differences Δ_i , $i = 1, \dots, N-1$, symmetric coupling $K_{-j} = K_j$ and even coupling function $g(x)$ is divergence free.*

Proof. We give the proof for the case (A), since the case (B) is analogous.

$$\begin{aligned} \text{div}G(\Phi) &= \sum_{i=1}^{N-1} \frac{\partial \dot{\varphi}_i}{\partial \varphi_i} = \sum_{i=1}^{[(N-1)/2]} K_i (g'(\varphi_i) - g'(\varphi_{-i})) \\ &+ \sum_{i=1}^{N-1} \left(\sum_{j=1}^{[(N-1)/2]} K_j (g'(\varphi_{i+j} - \varphi_i) - g'(\varphi_{i-j} - \varphi_i)) \right) \end{aligned}$$

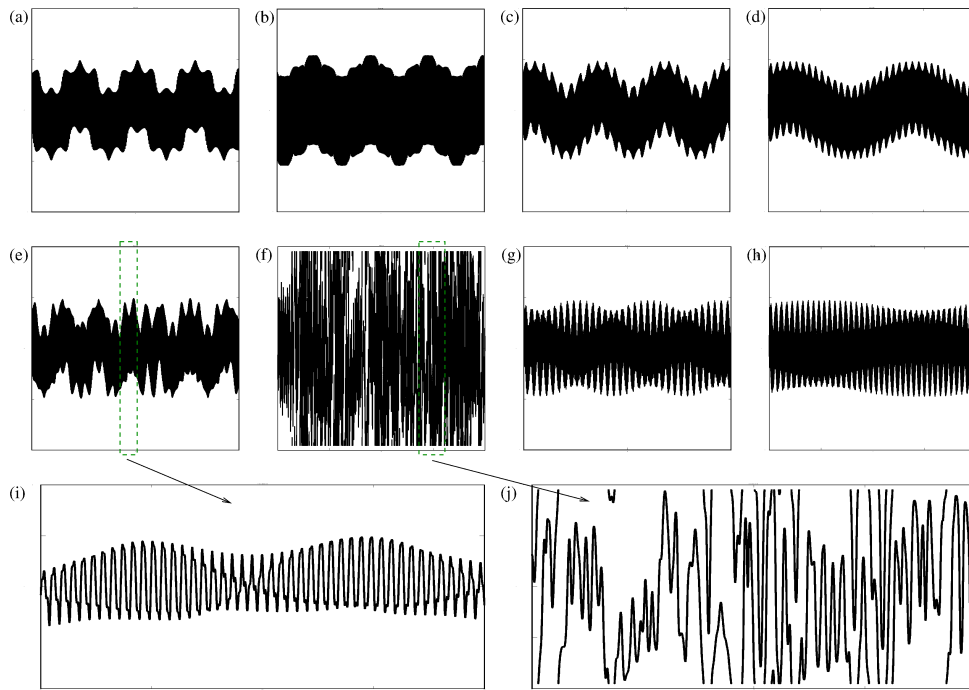


Figure 7.1: The coexistence of periodic, quasi-periodic, and chaotic solutions in the divergence-free system of seven phase oscillators with graph Fig. 2.1(b). Time series $(t, \varphi_1(t))$, $t \in [0, 2000]$, $\varphi_1 \in [-\pi, \pi]$, for $N = 7$, $l = 2$, $a = -b = -1$, $g(x) = -\sin(x)$. Initial conditions are different in different simulations.

$$\begin{aligned}
 &= \sum_{j=1}^{[(N-1)/2]} K_j \left(\sum_{i=0}^{N-1} (g'(\varphi_{i+j} - \varphi_i) - g'(\varphi_{i-j} - \varphi_i)) \right) \\
 &= \sum_{j=1}^{[(N-1)/2]} K_j \left(\sum_{i=0}^{N-1} (g'(\varphi_{i+j} - \varphi_i) - g'(\varphi_i - \varphi_{i+j})) \right) = 0,
 \end{aligned}$$

since $g'(x) = g'(-x)$ is implied by $g(x) = -g(-x)$. \square

Remark 19. We remark that a system of Kuramoto-Sakaguchi oscillators with the phase shift $\alpha = \pi/2$ is a particular situation of the case (B) of the Proposition 18.

The divergence-free system of coupled oscillators can demonstrate the coexistence of periodic, quasi-periodic, and chaotic behavior. Fig. 7.1 shows solutions of different types for different initial conditions and the same parameters. Homotopic to zero and non-homotopic to zero solutions coexist in phase space.

Proposition 20. *The system (6.2) with nearest neighbor coupling*

$$\dot{\varphi}_i = K_1(g(\varphi_1) - g(\varphi_{-1}) - g(\varphi_{i+1} - \varphi_i) + g(\varphi_{i-1} - \varphi_i))$$

and odd coupling function $g(\varphi)$ has the first integral

$$I_1(\varphi_1, \dots, \varphi_{N-1}) = \sum_{i=0}^{N-1} h(\varphi_i - \varphi_{i+1}),$$

where $h'(\varphi) = g(\varphi)$, $\varphi_N = \varphi_0 = 0$. We note that $h(\varphi)$ is even.

Proposition 21. Consider the system (6.2) with even oscillator number and odd coupling function $g(\varphi)$ with skew-symmetric coupling matrix ($K_j = -K_{-j}$) and $K_j = 0$ for even j , i.e. oscillators are coupled with the nearest neighbors, third neighbor, fifth neighbor, etc. This system has the first integral

$$I_2(\varphi_1, \dots, \varphi_{N-1}) = \sum_{i=1}^{N-1} (-1)^{i-1} \varphi_i.$$

7.2 Pairwise equidistant natural frequencies and reversibility

In this section we show that the general system (2.4) can have the reversibility property when the coupling is skew-symmetric and the frequencies are not identical, but satisfy a particular relation. System (2.4) for skew-symmetric coupling can be written as

$$\dot{\varphi}_i = \Delta_i + \sum_{j=1}^{[(N-1)/2]} K_j (g(\varphi_j) - g(\varphi_{-j}) - g(\varphi_{i+j} - \varphi_i) + g(\varphi_{i-j} - \varphi_i)), \quad (7.1)$$

where $i = 1, \dots, N - 1$, see also (6.2).

Proposition 22. System (7.1) is time-reversible with the involution \mathcal{R} determined by (6.3) if and only if the following relation between the frequency differences hold

$$\Delta_{N-i} = -\Delta_i, \quad i = 1, \dots, [N/2]. \quad (7.2)$$

Proof. We rewrite system (7.1) as

$$\dot{\varphi}_i = \tilde{G}_i(\varphi_1, \dots, \varphi_{N-1}) = \Delta_i + G_i(\varphi_1, \dots, \varphi_{N-1}), \quad i = 1, \dots, N - 1. \quad (7.3)$$

It holds

$$\tilde{G}_i(\mathcal{R}\Phi) = \Delta_i + G_i(\mathcal{R}\Phi) = -(-\Delta_i + G_{N-i}(\Phi))$$

and

$$-\tilde{G}_{N-i}(\Phi) = -(\Delta_{N-i} + G_{N-i}(\Phi)).$$

□

Remark 23. Note that Eq. (7.2) and, hence, conditions of Proposition 22 hold for the particular case of equally-distributed frequencies $\omega_j = \omega_0 + hj$ in the case of an odd number N of oscillators.

In this case it is easy to see that the reversibility condition (6.3) is satisfied if and only if (7.2) holds, that corresponds to pairwise equidistant distribution of frequency pairs around the frequency of the first oscillator: $(\omega_{i+1} + \omega_{N-i+1})/2 = \omega_1$. We remind that $\Delta_{N/2} = 0$ when N is even.

As a result of Proposition 22, the Hamiltonian-like dynamics appears in systems of non-identical oscillators that satisfy relation (7.2). Indeed, at least for small deviations Δ from zero, the families of periodic orbits that are mentioned in statement (A) of proposition 15 persist, since they appear due to the generic intersection of $\mathcal{F}_t(\text{Fix } \mathcal{R})$ and $\text{Fix } \mathcal{R}$. The dissipative equilibria remain also dissipative under small perturbations.

7.3 Non-homotopic to zero Hamiltonian-like part

A Hamiltonian-like dynamics of (7.1) that is non-homotopic to zero is possible when $|\Delta_i|$ are large enough. An example is shown in Fig. 5.2(o) for three oscillators, where such a region is foliated by periodic trajectories that are non-homotopic to zero. There might be a coexistence of the regions with homotopic to zero periodic orbits with another region filled with non-homotopic to zero periodic orbits, see yellow and green regions in Fig. 5.2(o). The coexistence of many regions of two types is also possible, as shown in Fig. 5.2(p) for $N = 3$ and coupling function (9.1).

Increasing frequency differences $|\Delta_i|$ from zero leads to a sequence of the disappearance of equilibria via local bifurcations. The homotopic to zero Hamiltonian-like part of the dynamics disappears together with the disappearance of the equilibrium within $\text{Fix } \mathcal{R}$. Then, a possible Hamiltonian-like part can consist only of non-homotopic to zero non-isolated orbits. Similar situations were observed for other systems in [60] and [59]. From this point of view, it is instructive to give conditions when the system does not possess equilibria.

Proposition 24. *System (7.1) does not have fixed points when one of the following conditions is satisfied:*

$$\min_{x \in \mathbb{T}^1} g(x) > -4[(N-1)/2] \min_i |\Delta_i|$$

or

$$\max_{x \in \mathbb{T}^1} g(x) < -4[(N-1)/2] \max_i |\Delta_i|.$$

Proof. The proof follows from the conditions $\Delta_i + \tilde{G}_i(\Phi) > 0$ (< 0) for $i = 1, \dots, [N/2]$. Note that the conditions of this proposition are satisfied when the frequency differences are large enough. \square

8 Large system ($N \rightarrow \infty$) and nonlinear Schrödinger amplitude equation for skew-symmetric coupling

In this section we consider the dynamics in a neighborhood of the synchronous solution $\theta_i = \theta$ in the case of an infinite chain of identical oscillators ($N \rightarrow \infty$) when each oscillator is coupled with a finite number $2l$ of its neighbors:

$$\dot{\theta}_i = \omega + \sum_{j=-l}^l K_j g(\theta_i - \theta_{i+j}), \quad i = 1, \dots, N, \quad (8.1)$$

and a *skew-symmetric* coupling matrix K , i.e. $K_j = -K_{-j}$, $j = 1, \dots, l$.

Using the "co-rotating" coordinates $\psi_i = \theta_i - \left(\omega + g(0) \sum_{j=-l}^l K_j \right) t$, system (8.1) is reduced to

$$\dot{\psi}_i = \sum_{j=-l}^l K_j f(\psi_i - \psi_{i+j}) \quad (8.2)$$

with $f(x) = g(x) - g(0)$. Since $f(0) = 0$, the one-dimensional invariant synchronization manifold

$$\mathcal{S} = \{(\psi_1, \dots, \psi_N) : \psi_i = \psi, i = 1, \dots, N\}$$

consists of equilibria $\psi_i = \psi = \text{const}$, which are related to each other by the phase-shift symmetry. Hence, the equilibria have neutral stability along the manifold and the same stability properties in the transverse directions to the manifold. Therefore, in order to study the dynamics in the neighborhood of a synchronous solution, it is enough to consider the neighborhood of the origin $\psi_i = 0, i = 1, \dots, N$. Note that in this section we do not write system for phase differences Eq. (2.4), but work directly with (8.2). This will result in the persistence of the phase-shift symmetry in the obtained amplitude equations.

Expanding function $f(x)$ in Taylor series, we rewrite system (8.2) as

$$\begin{aligned} \dot{\psi}_i = & \sum_{j=-l}^l Q_j \psi_{i+j} + \frac{f''(0)}{2f'(0)} \sum_{j=-l}^l Q_j (\psi_i - \psi_{i+j})^2 \\ & + \frac{f'''(0)}{6f'(0)} \sum_{j=-l}^l Q_j (\psi_i - \psi_{i+j})^3 + O(\|\psi\|^4) \end{aligned} \quad (8.3)$$

where

$$\begin{aligned} Q_0 &= f'(0) \sum_{j=-l, j \neq 0}^l K_j, \\ Q_j &= -K_j f'(0), \quad j = -l, \dots, l, j \neq 0. \end{aligned}$$

The Jacobi matrix Q is circulant and, similarly to Eq. (3.9), its eigenvalues are:

$$\lambda_m(Q) = \sum_{j=-l}^l Q_j e^{i2\pi jm/N}, \quad m = 1, \dots, N.$$

In the limit of large N , the spectrum can be approximated by the *asymptotic continuous spectrum* [68, 69]:

$$\begin{aligned} \lambda(\phi) = \sum_{j=-l}^l e^{ij\phi} Q_j = & Q_0 + \sum_{j=1}^l (Q_j + Q_{-j}) \cos(j\phi) \\ & + i \sum_{j=1}^l (Q_j - Q_{-j}) \sin(j\phi), \quad \phi \in [0, 2\pi). \end{aligned} \quad (8.4)$$

with a continuous parameter $0 \leq \phi \leq 2\pi$. Each function $\lambda(\phi)$ presents a closed curve in the complex plane \mathbb{C} . Using (8.4) and definition of Q_j , one can check that $\lambda(0) = 0$, that corresponds to the neutral stability along the invariant manifold \mathcal{M} . Expression (8.4) implies also the symmetry of spectrum $\lambda(-\phi) = \overline{\lambda(\phi)}$.

The skew-symmetry of matrix K implies the skew-symmetry of the matrix Q : $Q_j = -Q_{-j}$. Therefore,

$$\lambda(\phi) = i2 \sum_{j=1}^l Q_j \sin(j\phi) = i\tilde{\omega}(\phi), \quad \tilde{\omega}(\phi) \in \mathbb{R},$$

and the whole spectrum belongs to the interval $[-i \max_{\phi} \tilde{\omega}(\phi), i \max_{\phi} \tilde{\omega}(\phi)]$ of the imaginary axis.

Assuming that the coupling function has a *cubic nonlinearity* and using the approach from [29], adapted to the spatially discrete case as proposed in [22, 68], the following statement holds.

Proposition 25. Assume that system (8.3) satisfies the following conditions:

- 1) the coupling matrix is skew-symmetric : $Q_j = -Q_{-j}$;
- 2) there exists $\phi_0 \neq 0$ such that $\tilde{\omega}(\phi_0) \neq 0$;
- 3) the coupling function has a cubic nonlinearity at zero, i.e. $f'''(0) = 0$;
- 4) the second derivative of the imaginary part is not equal to zero: $\tilde{\omega}''(\phi_0) \neq 0$;
- 5) non-resonance condition: $\sum_{j=1}^l Q_j \sin^3(j\phi_0) \neq 0$.

Let $\varepsilon = 1/N$. Then the multiple scale ansatz

$$\psi_i(t) = \varepsilon \mathcal{A}(T_1, x_i, T_2) e^{i(\omega_0 t + \phi_0 i)} + \varepsilon^3 \mathcal{A}^3(T_1, x_i, T_2) e^{3i(\omega_0 t + \phi_0 i)} v_3 + c.c., \quad (8.5)$$

with the amplitude $\mathcal{A} \in \mathbb{C}$ depending on the rescaled coordinates $T_1 = \varepsilon t$, $T_2 = \varepsilon^2 t$, and $x_i = \varepsilon i$ (c.c. denotes complex conjugated terms, $v_3 \in \mathbb{R}$) to system (8.3) leads to the following solvability conditions up to the order ε^3 :

$$i\partial_{T_2} u = \frac{1}{2} \tilde{\omega}''(\phi_0) \partial_\xi^2 u + \rho u |u|^2, \quad (8.6)$$

with periodic boundary conditions

$$u(\xi, T_2) = u(\xi + 1, T_2),$$

where $u(\xi, T_2)$ with $\xi \in [0, 1]$ is related to the amplitude \mathcal{A} by

$$\mathcal{A}(T_1, x_i, T_2) = u(\tilde{\omega}'(\phi_0) T_1 + x_i, T_2)$$

and

$$\rho = \frac{2f'''(0)}{f'(0)} \sum_{j=1}^l Q_j \sin(j\phi_0) (\cos(j\phi_0) - 1).$$

Remark 26. Note that the amplitude has to satisfy the nonlinear Schrödinger equation (8.6), which is Hamiltonian. This confirms that the skew-symmetric coupling leads to the Hamiltonian dynamics in the vicinity of the synchronous solution of the chain.

9 Discussion

In this concluding section we point out some general consequences of our results.

(i) *Unidirectional rings are special case of anisotropic coupling:* The case when the ring is unidirectional is important for applications and considered in many works, see e.g. [14, 37, 69, 42, 10, 57, 46]. The general network (2.1) is unidirectional when $K_i \neq 0$ for $j = 1, \dots, [(N-1)/2]$ and $K_j = 0$ in other cases. For the forward-backward system (4.1) the condition for unidirectionality is just $b = 0$. The bifurcation diagram Fig. 5.1 shows that the system dynamics does not change qualitatively with a small variation of coupling parameters. Actually, one can see that the straight line $b = 0$ and lines $b = \pm\varepsilon$ intersect bifurcation lines (AH, HC, TC) transversally at almost the same points when ε is close to zero. This tells us about the structural stability of the system along parametric line $b = 0$ independently on parameter α .

(ii) *Effects of higher harmonics in the coupling function:* In Sec. 5 we considered examples where the coupling function had only the first term of the Fourier series (5.1). If the coupling function has higher harmonics, the basic properties related to the symmetries or reversibility of the system remain the

same. However, a more complex shape of $g(x)$ can lead to the appearance of new solutions or new bifurcation properties. For instance, for the Hansel-Mato-Meunier coupling function [25]

$$g(x) = -\sin(x - \alpha) + p \sin(2x) \quad (9.1)$$

the system (2.4) has additional fixed points when $|p| \geq 1/2$. If these additional points belong to $\text{Fix } \mathcal{R}$, there might appear the same Hamiltonian-like regions around them, similar as it is described above.

An example in Fig. 5.2(m) shows that the system of three coupled oscillators with function (9.1) has four different Hamiltonian-like regions: three of them are bounded by homoclinic loops (colored regions in Fig. 5.2(m)) and one is bounded by a Z_3 -heteroclinic cycle. These regions coexist with the simply connected dissipative region that includes the sink \mathcal{M}_1 , the source \mathcal{M}_2 , and heteroclinic trajectories that connect these two points. Figures 5.2(n), (o), and (p) illustrate other possible examples. In particular, Fig. 5.2(o) shows how two Hamiltonian-like regions coexist, one of which is homotopic and another is non-homotopic to zero.

Acknowledgments

We thank L. Recke, M. Zaks, A. Pikovsky, M. Rosenblum and P. Ashwin for useful discussions.

References

- [1] D.M. Abrams and S.H. Strogatz. Chimera states for coupled oscillators. *Phys. Rev. Lett.*, 93.:174102, 2004.
- [2] G. E. Alexander, M. R. DeLong, and P. L. Strick. Parallel organization of functionally segregated circuits linking basal ganglia and cortex. *Annu. Rev. Neurosci.*, 9:357–381, 1986.
- [3] V.I. Arnold. Reversible systems. *Nonlinear and Turbulent Processes in Physics*, 3:1161–1174, 1984. Nonlinear and turbulent processes in physics; Proceedings of the Second International Workshop, Kiev, Ukrainian SSR, October 10-25, 1983. Volume 3 (A85-28566 12-70). Chur, Switzerland and New York, Harwood Academic Publishers.
- [4] V.I. Arnol'd and M.B. Sevryuk. Oscillations and bifurcations in reversible systems. *In: Nonlinear Phenomena in Plasma Physics and Hydrodynamics*, ed.R. Z. Sagdeev, Mir, Moscow, pages 31–64, 1986.
- [5] A. Back, J. Guckenheimer, M.R. Myers, F.J. Wicklin, and P.A. Worfolk. DsTool: Computer assisted exploration of dynamical systems. *Notices Amer. Math. Soc.*, 39(4):303–309, 1992.
- [6] Wei Baoshe. Perturbations of lower dimensional tori in the resonant zone for reversible systems. *Journal of Mathematical Analysis and Applications*, 253(2):558–577, 2001.
- [7] Igor Belykh and Andrey Shilnikov. When weak inhibition synchronizes strongly desynchronizing networks of bursting neurons. *Physical Review Letters*, 101(7):078102, 2008.
- [8] Michele Bonnin. Waves and patterns in ring lattices with delays. *Physica D: Nonlinear Phenomena*, 238(1):77 – 87, 2009.

- [9] Hadrien Bosetti, Harald A. Posch, Christoph Dellago, and William G. Hoover. Time-reversal symmetry and covariant Lyapunov vectors for simple particle models in and out of thermal equilibrium. *Phys. Rev. E*, 82:046218, Oct 2010.
- [10] Barbara J. Breen, Aaron B. Doud, Jamie R. Grimm, Andrew H. Tanasse, Stuart J. Tanasse, John F. Lindner, and Katsuo J. Maxted. Electronic and mechanical realizations of one-way coupling in one and two dimensions. *Phys. Rev. E*, 83:037601, Mar 2011.
- [11] H. W. Broer, M. C. Ciocci, and Heinz Hanssmann. The quasi-periodic reversible Hopf bifurcation. *International Journal of Bifurcation and Chaos*, 17(8):2605–2623, 2007. Relation: <http://www.rug.nl/informatica/organisatie/overorganisatie/iwi> Rights: University of Groningen. Research Institute for Mathematics and Computing Science (IWI).
- [12] H. W. Broer, G. B. Huitema, and M. B. Sevryuk. *Quasi-Periodic Motions in Families of Dynamical Systems*. Springer, 1996.
- [13] H.W. Broer, G.B. Huitema, and M.B. Sevryuk. Families of quasi-periodic motions in dynamical systems depending on parameters. *Progress in nonlinear differential equations and their applications*, 19:171–211, 1996.
- [14] A. Bulsara, V. In, A. Kho, P. Longhini, A. Palacios, W. Rappel, J. Acebron, S. Baglio, and B. Ando. Complex behavior in driven unidirectionally coupled overdamped duffing elements. *Phys. Rev. E*, 73(6):066121, Jun 2006.
- [15] J.J. Collins and I. Stewart. A group-theoretic approach to rings of coupled biological oscillators. *Biol Cybern*, 71(2):95–103, 1994.
- [16] H. Daido. Strange waves in coupled-oscillator arrays: Mapping approach. *Phys. Rev. Lett.*, 78(9):1683–1686, 1997.
- [17] Guy Van der Sande, Miguel C. Soriano, Ingo Fischer, and Claudio R. Mirasso. Dynamics, correlation scaling, and synchronization behavior in rings of delay-coupled oscillators. *Physical Review E (Statistical, Nonlinear, and Soft Matter Physics)*, 77(5):055202, 2008.
- [18] R.L. Devaney. Reversible diffeomorphisms and flows. *Trans. Am. Math. Soc.*, 218:89–113, 1976.
- [19] Eusebius J. Doedel. *AUTO-07P: Continuation and bifurcation software for ordinary differential equations*. Montreal, Canada, April 2006.
- [20] B Fiedler and D Turaev. Coalescence of reversible homoclinic orbits causes elliptic resonance. *INTERNATIONAL JOURNAL OF BIFURCATION AND CHAOS*, 6:1007–1027, 1996.
- [21] Jean-Jacques Gervais. Bifurcations of subharmonic solutions in reversible systems. *Journal of Differential Equations*, 75(1):28–42, 1988.
- [22] Johannes Giannoulis and Alexander Mielke. The nonlinear Schrödinger equation as a macroscopic limit for an oscillator chain with cubic nonlinearities. *Nonlinearity*, 17:551–565, 2004.
- [23] Martin Golubitsky, Martin Krupa, and Chjan Lim. Time-reversibility and particle sedimentation. *SIAM Journal on Applied Mathematics*, 51(1):49–72, 1991.
- [24] Martin Golubitsky and William F Langford. Classification and unfoldings of degenerate Hopf bifurcations. *Journal of Differential Equations*, 41(3):375–415, 1981.

- [25] D. Hansel, G. Mato, and C. Meunier. Clustering and slow switching in globally coupled phase oscillators. *Phys. Rev. E*, 48(5):3470–3477, November 1993.
- [26] F. C. Hoppensteadt and E. M. Izhikevich. *Weakly connected neural networks*, volume 126 of *Applied Mathematical Sciences*. Springer-Verlag, New York, 1997.
- [27] M. Kantner and S. Yanchuk. Bifurcation analysis of delay-induced patterns in a ring of Hodgkin-Huxley neurons. *Phil. Trans. Roy. Soc. A*, 371:20120470, 2013.
- [28] Tomasz Kapitaniak, Patrycja Kuzma, Jerzy Wojewoda, Krzysztof Czołczynski, and Yuri Maistrenko. Imperfect chimera states for coupled pendula. *Scientific Reports*, 4:6379–, September 2014.
- [29] P. Kirrmann, G. Schneider, and A. Mielke. The validity of modulation equations for extended systems with cubic nonlinearities. *Proc. Roy. Soc. Edinburgh Sect. A*, 122:85–91, 1992.
- [30] Vladimir Klinshov, Dmitry Shchapin, Serhiy Yanchuk, and Vladimir Nekorkin. Jittering waves in rings of pulse oscillators. *Phys. Rev. E*, 94:012206, 2016.
- [31] Y. Kuramoto. *Chemical Oscillations, Waves, and Turbulence*. Springer, Berlin, 1984.
- [32] Yoshiki Kuramoto and Dorjsuren Battogtokh. Coexistence of coherence and incoherence in non-locally coupled phase oscillators. *Nonlinear Phenomena in Complex Systems*, 5(4):380–385, 2002.
- [33] J S W Lamb. Reversing symmetries in dynamical systems. *Journal of Physics A: Mathematical and General*, 25(4):925, 1992.
- [34] Jeroen S. W. Lamb and Mark Roberts. Reversible equivariant linear systems. *J. Differential Equations*, 159:279, 1998.
- [35] Jeroen S.W. Lamb and John A.G. Roberts. Time-reversal symmetry in dynamical systems: A survey. *Physica D*, 112:1–39, 1998.
- [36] Jeroen S.W. Lamb and Claudia Wulff. Reversible relative periodic orbits. *Journal of Differential Equations*, 178(1):60–100, 2002.
- [37] John F. Lindner, Kelly M. Patton, Patrick M. Odenthal, James C. Gallagher, and Barbara J. Breen. Experimental observation of soliton propagation and annihilation in a hydromechanical array of one-way coupled oscillators. *Phys. Rev. E*, 78:066604, Dec 2008.
- [38] I. P. Marino, V. Pérez-Muñuzuri, V. Pérez-Villar, E. Sánchez, and M. A. Matías. Interaction of chaotic rotating waves in coupled rings of chaotic cells. *Phys. D*, 128(2-4):224–235, 1999.
- [39] J. Moser. *Stable and Random Motions in Dynamical Systems*. Princeton Univ. Press, Princeton, 1973.
- [40] I. O. Parasyuk. Conservation of quasiperiodic motions of reversible multifrequency systems. *Dokl. Akad. Nauk Ukrain. SSR*, A 9:19–22, 1982. In Russian.
- [41] P. Perlikowski, S. Yanchuk, O. V. Popovych, and P. A. Tass. Periodic patterns in a ring of delay-coupled oscillators. *Phys. Rev. E*, 82(3):036208, Sep 2010.

- [42] P. Perlikowski, S. Yanchuk, M. Wolfrum, A. Stefanski, P. Mosiolek, and T. Kapitaniak. Routes to complex dynamics in a ring of unidirectionally coupled systems. *Chaos*, 20:013111, 2010.
- [43] Arkady Pikovsky and Philip Rosenau. Phase compactons. *Physica D: Nonlinear Phenomena*, 218(1):56 – 69, 2006.
- [44] A. Politi, G. L. Oppo, and R. Badii. Coexistence of conservative and dissipative behavior in reversible dynamical systems. *Phys. Rev. A*, 33:4055–4060, Jun 1986.
- [45] O. V. Popovych, S. Yanchuk, and P. A. Tass. Delay- and coupling-induced firing patterns in oscillatory neural loops. *Phys. Rev. Lett.*, 107:228102, 2011.
- [46] S Rajamani and S Rajasekar. Signal amplification by unidirectional coupling of oscillators. *Physica Scripta*, 88(1):015010, 2013.
- [47] Liwei Ren and Bard Ermentrout. Phase locking in chains of multiple-coupled oscillators. *Physica D: Nonlinear Phenomena*, 143(1–4):56 – 73, 2000.
- [48] M R Ricard. On degenerate planar hopf bifurcations. *Journal of Physics A: Mathematical and Theoretical*, 44(6):065202, 2011.
- [49] J. A. G. Roberts and G. R. W. Quispel. Chaos and time-reversal symmetry: Order and chaos in reversible dynamical systems. *Phys. Rep.*, 216:63–177, 1992.
- [50] H. Sakaguchi and Y. Kuramoto. A soluble active rotator model showing phase transitions via mutual entrainment. *Prog Theor Phys*, 76:576–581, 1986.
- [51] E. Sánchez and M. A. Matías. Experimental observation of a periodic rotating wave in rings of unidirectionally coupled analog lorenz oscillators. *Phys. Rev. E*, 57(5):6184–6186, May 1998.
- [52] M.B. Sevryuk. *Reversible Systems*. Springer Lecture Notes in Mathematics. Springer, Berlin, 1986.
- [53] M.B. Sevryuk. On invariant tori of reversible systems in the neighbourhood of an equilibrium position. *Russian Math. Surveys*, 42(4):147–148, 1987.
- [54] Mikhail B. Sevryuk. The reversible context 2 in kam theory: the first steps. *Regular and Chaotic Dynamics*, 16:24–38, 2011.
- [55] Andrey Shilnikov, René Gordon, and Igor Belykh. Polyrhythmic synchronization in bursting networking motifs. *Chaos*, 18(3):037120, 2008.
- [56] Miguel C. Soriano, Jordi Garcia-Ojalvo, Claudio R. Mirasso, and Ingo Fischer. Complex photonics: Dynamics and applications of delay-coupled semiconductor lasers. *Rev. Mod. Phys.*, 85:421–470, 2013.
- [57] Natalja Strelkova and Mauricio Barahona. Transient dynamics around unstable periodic orbits in the generalized repressilator model. *Chaos*, 21(2):–, 2011.
- [58] A. Takamatsu, R. Tanaka, H. Yamada, T. Nakagaki, T. Fujii, and I. Endo. Spatiotemporal symmetry in rings of coupled biological oscillators of physarum plasmodial slime mold. *Phys. Rev. Lett.*, 87(7):078102, Jul 2001.

- [59] Dmitri Topaj and Arkady Pikovsky. Reversibility vs. synchronization in oscillator lattices. *Physica D: Nonlinear Phenomena*, 170(2):118–130, 2002.
- [60] Kwok Yeung Tsang, Renato E. Mirollo, Steven H. Strogatz, and Kurt Wiesenfeld. Dynamics of a globally coupled oscillator array. *Physica D: Nonlinear Phenomena*, 48(1):102–112, 1991.
- [61] Kwok Yeung Tsang, Renato E. Mirollo, Steven H. Strogatz, and Kurt Wiesenfeld. Reversibility and noise sensitivity of josephson arrays. *Phys. Rev. Lett.*, 66:1094–1097, Feb 1991.
- [62] Guy Van der Sande, Miguel C. Soriano, Ingo Fischer, and Claudio R. Mirasso. Dynamics, correlation scaling, and synchronization behavior in rings of delay-coupled oscillators. *Phys. Rev. E*, 77:055202, 2008.
- [63] A. Vanderbauwhede. *Local Bifurcation and Symmetry*, volume 75 of *Research Notes in Mathematics*. Pitman, London, 1982.
- [64] A.T. Winfree. *The geometry of biological time*. Springer, 2001.
- [65] Jeremy Wojcik, Justus Schwabedal, Robert Clewley, and Andrey L. Shilnikov. Key bifurcations of bursting polyrhythms in 3-cell central pattern generators. *PLoS ONE*, 9(4):e92918, 2014.
- [66] M. Wolfrum, O. E. Omel'chenko, S. Yanchuk, and Y. L. Maistrenko. Spectral properties of chimera states. *Chaos*, 21(1):013112, 8, 2011.
- [67] S. Yanchuk, P. Perlikowski, O. V. Popovych, and P. A. Tass. Variability of spatio-temporal patterns in non-homogeneous rings of spiking neurons. *Chaos*, 21:047511, 2011.
- [68] S. Yanchuk, P. Perlikowski, M. Wolfrum, A. Stefanski, and T. Kapitaniak. Amplitude equations for collective spatio-temporal dynamics in arrays of coupled systems. *Chaos: An Interdisciplinary Journal of Nonlinear Science*, 25(3):033113, 2015.
- [69] S. Yanchuk and M. Wolfrum. Destabilization patterns in chains of coupled oscillators. *Phys. Rev. E*, 77(2):026212, 2008.
- [70] Ying Zhang, Gang Hu, and Hilda A. Cerdeira. How does a periodic rotating wave emerge from high-dimensional chaos in a ring of coupled chaotic oscillators? *Phys. Rev. E*, 64(3):037203, Aug 2001.
- [71] Zhengyu Zhang. Reducibility of reversible system with small perturbation. *Ann. Differ. Equations*, 21(4):629–638, 2005.